Unsteady Peristaltic Flow with the Interaction of Nanoparticles

Name: Ayesha Ayub

Reg. # 00000117018

This thesis is submitted as a partial fulfillment of the requirements for the degree of
Master of Science in
Mathematics

Supervised by: Dr. Noreen Sher Akbar

Department of Mathematics

School of Natural Sciences (SNS)

National University of Sciences and Technology (NUST)
H-12, Islamabad, Pakistan

2017

National University of Sciences & Technology

MASTER'S THESIS WORK

We hereby recommend that the dissertation prepared under our supervision by: Ms. Ayesha Ayub, Regn No. 00000117018 Titled: Unsteady Peristaltic flow with the Interaction of Nanoparticles be accepted in partial fulfillment of the requirements for the award of **MS** degree.

Examination Committee Members

1. Name: DR. MERAJ MUSTAFA HASHMI   Signature: _____

2. Name: DR. ASIM AZIZ   Signature: _____

3. Name: _____   Signature: _____

External Examiner : DR. SOHAIL NADEEM   Signature: _____

Supervisor's Name: DR. NOREEN SHER AKBAR   Signature: _____

_____
Head of Department

10-01-18
Date

COUNTERSINGED

Date: 10-01-18

_____
Dean/Principal

THESIS ACCEPTANCE CERTIFICATE

Certified that final copy of MS thesis written by **Ms. Ayesha Ayub**, (Registration No. **00000117018**), of **School of Natural Sciences** has been vetted by undersigned, found complete in all respects as per NUST statutes/regulations, is free of plagiarism, errors, and mistakes and is accepted as partial fulfillment for award of MS/M.Phil degree. It is further certified that necessary amendments as pointed out by GEC members and external examiner of the scholar have also been incorporated in the said thesis.

Signature: _____

Name of Supervisor Dr. Noreen Sher Akbar

Date: _____ 10.01.18

Signature (HoD): _____

Date: _____ 10-01-18

Signature (Dean/Principal): _____

Date: _____ 10-01-18

In the name of ALLAH, the Gracious, the Merciful

Dedicated to

My beloved parents Muhammad Ayub, Sabira Parveen and my siblings Ubaid Ur Rehman, Javeria and Maria Ayub.

Acknowledgements

First of all, I would like to thank **Allah Almighty**, who has given me the ability, courage and His blessings to complete this thesis. He gave me strength and right path throughout my research work.

My special and sincere thanks to my supportive supervisor, **Dr. Noreen Sher Akbar** for providing me the most peaceful environment to work and guiding me throughout my research work. A special thanks to my guidance and evaluation committee members, **Dr. Meraj Mustafa** and **Dr. Asim Aziz**, for their valuable guidance, suggestions and encouragement. I am grateful especially to **School of Natural Sciences**, **NUST** for providing me all the facilities and a platform to work. I greatly acknowledge the facilities and technical support provided by other schools of NUST.

Finally, I would like to convey my gratitude to all friends for their help, guidance and prayers. I would like to thank my family especially my father **Muhammad Ayub,** my mother **Sabira Parveen,** uncle **Nazir Ali Zaidi** and my friend **Sidra Yousaf** for being so supportive and for their love.

Ayesha Ayub

Abstract

Carbon nanotubes analysis is done for an unsteady physiological flow in a non-uniform channel of finite length. For the non-dimensional governing equations subject to physically realistic boundary conditions, exact solutions are acquired. The effects of carbon nanotubes on effective thermal conductivity, axial velocity, transverse velocity, temperature, and pressure difference distributions along the length of non-uniform channel by varying the flow parameters, are studied with the help of graphs plotted on Mathematica. Trapping is also studied. We observed that Multi walled carbon nanotubes have this exceptional quality to increase the axial velocity as well as the transverse velocity of the governing fluids.

Contents

Chapter 1

Introduction

Peristalsis is the process of muscle contractions and expansions in a wave-like fashion. It is the reflexive movements of the longitudinal and disc-shaped muscles which move the food in the digestive tract and other vacant tubes of the body. This phenomenon of peristalsis arises in the esophagus and intestines which initiates when a food bolus is consumed. In 1969, Shapiro AH [1] studied the fluid movements by considering long wavelengths throughout the peristaltic pumping. Abstract results are shown for plane and axis symmetric geometries. The theoretical pressure decreases in a linear way with an increase in time-mean flow, for a considered amplitude ratio. Calculation of the specific fluid motions show that the net time is algebraic difference among the forward time-mean flow which is at the interior tube and the backward time-mean flow which is close to the periphery of the tube. This research opened new horizons for researchers to study peristalsis under different circumstances. Radhakrishnamacharya G [2] has considered the channel having two dimensions, power law fluid is examined by her which is moving peristaltically. By assuming that the peristaltic wavelength is greater than the mean half-width of the channel. The output for the stream function is acquired as an asymptotic growth. The influence of the flow behavior index over the shear stress and streamline pattern is observed. Srivastava LM [3] investigated the flow of couple stress fluid across the stenotic blood vessels. By the study it is observed that by fixing stenosis size, there is an increase in shear stress and flow resistance when couple stress is decreased from unity. A detailed study on the peristaltic flow inside the human body was given by Pozrikidis [4]. A new study on the unsteady peristaltic transport in limited length tubes was first given by Li and Brasseur [5]. The peristaltic transport is migrating because of the sinusoidal wave through the boundary of incompressible filled fluid tube. The solution is acquired by taking zero Reynold number and by considering infinite wavelength. Several interesting articles on the peristaltic flow with applications in drug delivery, bacterial growth and clot blood model are presented in references [6-9]. The drug which is delivered via permeable

medium in a peristaltic blood flow of nanofluid is discussed. Perturbation method is used to get the analytic solution for temperature profiles, frictional force and nanoparticle concentration profiles. The impact of flow and peristaltic merging on increase in the number of bacteria in the gut, is modelled by a channel by arranging the membrane valves which basically permits colonic wall contraction. The bacterial profile shows changing spatial reliance, which is relying on the rate of flow and frequency of contractions. In the last case heat transfer has been observed on the clot blood model with variable viscosity. The peristaltic motion generates the propagation of blood along the annulus. This clot blood model is made by using the lubrication approach.

Recent advancements in fluid mechanics combined the studies of the nanofluids with peristaltic motion. Nanofluids are fluids containing nanoparticles, which are basically suspended in a base fluid. Nano fluids are well known for their vast applications in engineering, bio-medical sciences and industry. Nanofluids act as coolants in radiators because of their enhanced thermal properties [10-14]. Akbar and Butt [13] have done the investigation on heat transfer on the movement of copper nanofluids. Where numbers of cilia work simultaneously in such a way that generate waves to convey the fluid to finite length tube. Akbar NS, Butt AW [14] have also inspected the peristaltic movement of copper nanofluids in a bended channel with controllable walls. The exact solution is acquired by considering long wavelength approximation, for temperature profile and velocity of the fluid [14]. Khaliq and Kafafy [15] have done their work on increasing the effectiveness of polymerase chain reaction by using graphene Nano flakes. Mahian and kianifar [16] have done the analysis on the practical uses of nanofluids in solar energy. Nanofluids as liquid mixture are brought into service with nanometer-sized suspended solid particles. The impacts of nanofluids in the functioning of solar collectors and solar water heaters are observed. Some proposals are made to use nanofluids in various photovoltaics, solar thermoelectric cells and also in thermal systems.

The nanoparticles utilized in nanofluids are usually prepared of carbon nanotubes (Cnt's), made by dense sheets of carbon having a minor length-to-diameter ratio. These nanotubes have empty cylindrical nanostructures with the walls. They are widely used in the industry for their improved thermal conductivity, mechanical and electrical properties. Cnt's also have applications as preservatives in different structural materials containing the segments of cars. These carbon nanotubes are categorized as single-walled nanotubes (SWCnt's) and multi-walled nanotubes (MWCnt's). SWCnt's have a diameter near to 1 nanometer. MWCnt's are multiple nanotubes

having common center, exactly nested within one another. Its separate shells can be narrated as SWCnt's. These nanotubes have semiconductor behavior and are used in the progress of intermolecular field-effect transistors. Akbar and Butt [17-18] have studied various properties of Cnt's in different geometries and boundary conditions but the unsteady flow has not been studied in this direction. Recent studies associated to the topic are cited in Refs: [19-24]. Over the entropy generation Ellahi R [21] has examined the shape impacts of nanosize particles which are present in Cu- H_2O nanofluid. Mathematical model is studied to see the convection boundary layer flow adjacent to the cone which is inverted. He examined the impacts of porous medium, radiation and power law index. Nonlinear equations are solved analytically with the assumption of Bousinessq approximations. Ellahi R [24] has examined the model which is based on the Nano layer single and multi-wall carbon nanotubes hanged in salt water solutions to study the natural convection MHD nanofluids. BVPh 2.0 for solving the nonlinear partial differential equations. Motivated from the above researches and to fill the void, we have studied the unsteady flow of MWCnt's in a non-uniform medium. The governing flow equations are made dimension less and solved to find the analytical solutions of the velocity, temperature and pressure profiles. Results are analyzed with graphical illustrations, streamlines for the flow are also plotted.

Chapter 2

Preliminaries

2.1   Fluid

A fluid is a substance that faces continuous deformation when a shear stress is exerted on it. Fluid is classified into two main groups.

    (1) Liquids.

    (2) Gases.

2.2   Types of Flow

Some types of flows are:

    (1) Compressible flow.

    (2) Incompressible flow.

2.2.1 Compressible flow

By changing pressure or volume of the fluid, the density or volume of the fluid changes then the fluid is said to be compressible.

2.2.2 Incompressible flow

If there is no change in density or volume of the fluid when the pressure or volume of the fluid changes then the fluid is said to be incompressible.

2.3   Two-dimensional flow

The two-dimensional flow is one in which the variation of flow characteristics can be described by two spatial coordinates. At each point, the velocity of a flow is parallel to a static plane.

2.4   Nanofluid

The fluids possess nanoscale colloidal suspensions are called Nano fluids. Nano fluid basically contains two parts, nanoparticles and base fluids.

2.5   Nanoparticles

Nanoparticles are the particles between 1 to 100 nanometer in size. Common nanoparticles are carbon nanotubes, cerium oxide, titanium dioxide and nano silver.

2.6   Base fluids

The base fluids are the fluids in which nanoparticles are to be suspended. Some base fluids are water, oil, ethylene glycol etc.

2.7   Thermal capacitance

It is measure of temperature variation in a material based on its volume. It is also known as the ability of a material to store heat.

2.8   Prandtl number

Prandtl number is the ratio of kinematic viscosity to thermal diffusivity.

2.9   Convection

This process occurs when there is a change in temperature among two parts of a fluid. The hot part of fluid moves upward and the cooler part drops down. It happens because the hot water is less dense than cold water. Convection occurs only in fluids (liquids and gases).

2.10 Reynolds number

Reynolds number is the dimensionless number which is the ratio of inertial forces to viscous forces. It computes whether the fluid is streamlined, steady or unsteady, laminar or turbulent.

2.11 Thermal expansion

A change in shape, area or volume of a material in a reaction to change in the temperature is called thermal expansion.

2.12 Brownian motion

Brownian motion occurs when fast moving atoms or molecules in the gas or liquid collide with the suspended particles in a fluid.

Chapter 3

A Study on Peristaltic Flow of Nanofluids.

3.1. Introduction:

In this chapter the peristaltic flow of nanofluids via two dimensional channel is studied. The investigation is done by considering the long wavelength and low Reynolds number approximations. The walls of the channel surface propagate sinusoidally along the channel. The flow geometry is taken as a uniform channel of finite length. Buongiorno formulation for Nano fluids is used. Approximate analytical solutions for nanoparticle fraction field, temperature field, axial velocity, volume flow rate, pressure gradient and stream function are acquired. The effects of thermal Grashof number, Brownian motion parameter, thermophoresis parameter and basic-density Grashof number on nanoparticle fraction profile, temperature profile, velocity profile and also the trapping phenomenon is computed numerically.

3.2. Mathematical Model:
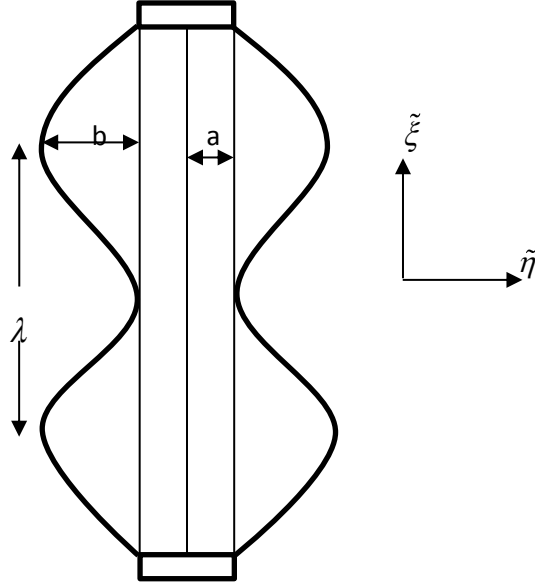
Fig. 3.1. Geometry of the peristaltic channel flow pattern.

In this chapter we consider the peristaltic flow of nanofluids across a uniform and two dimensional channel. The equation for the wall of geometry due to the propagation of train of waves can be written as:

$$\tilde{h}(\tilde{\xi},\tilde{t}) = a + b\sin\frac{2\pi}{\lambda}(\tilde{\xi} - c\tilde{t}),$$ (3.1)

$\tilde{h}$ is the transverse vibration of the wall , $\tilde{t}$ represents time and $\tilde{\xi}$ represents the axial coordinate. Whereas a is the half width of the channel, b is amplitude of the wave, λ is the wavelength and c is the wave velocity. The channel flow is examined where the surface of the wall has sinusoidal wave form. The values of the temperature at the center line and at the channel's wall are T_0 and T_1. The values of nanoparticle fraction at the center line and at the channel's wall are F_0 and F_1 respectively. Applying the Oberbeck-Boussinesq approximation and by taking up the most relevant practical case in which reference temperature is appropriate and dilute concentration of nanoparticles is taken. The ruling equation for the conservation of mass, momentum, thermal energy and nanoparticle fraction from refs: [30, 38, 39] can be set out as:

$$\frac{\partial \tilde{u}}{\partial \tilde{\xi}} + \frac{\partial \tilde{v}}{\partial \tilde{\eta}} = 0, \tag{3.2}$$

$$\rho_f \left(\frac{\partial}{\partial \tilde{t}} + \tilde{u}\frac{\partial}{\partial \tilde{\xi}} + \tilde{v}\frac{\partial}{\partial \tilde{\eta}} \right)\tilde{u} = -\frac{\partial \tilde{p}}{\partial \tilde{\xi}} + \mu\left(\frac{\partial^2 \tilde{u}}{\partial \tilde{\xi}^2} + \frac{\partial \tilde{u}^2}{\partial \tilde{\eta}^2} \right) + g[(1-F_0)\rho_{fo}\beta(T-T_0) - (\rho_p - \rho_{f0})(F-F_0)] \tag{3.3}$$

$$\rho_f \left(\frac{\partial}{\partial \tilde{t}} + \tilde{u}\frac{\partial}{\partial \tilde{\xi}} + \tilde{v}\frac{\partial}{\partial \tilde{\eta}} \right)\tilde{v} = -\frac{\partial \tilde{p}}{\partial \tilde{\xi}} + \mu\left(\frac{\partial^2 \tilde{v}}{\partial \tilde{\xi}^2} + \frac{\partial \tilde{v}^2}{\partial \tilde{\eta}^2} \right) + g[(1-F_0)\rho_{fo}\beta(T-T_0) - (\rho_p - \rho_{f0})(F-F_0)], \tag{3.4}$$

$$(\rho c)_f \left(\frac{\partial}{\partial \tilde{t}} + \tilde{u}\frac{\partial}{\partial \tilde{\xi}} + \tilde{v}\frac{\partial}{\partial \tilde{\eta}} \right)T = k\left(\frac{\partial^2 T}{\partial \tilde{\xi}^2} + \frac{\partial^2 T}{\partial \tilde{\eta}^2} \right) + (\rho c)_p \left\{ D_B\left(\frac{\partial F}{\partial \tilde{\xi}}\frac{\partial T}{\partial \tilde{\xi}} + \frac{\partial F}{\partial \tilde{\eta}}\frac{\partial T}{\partial \tilde{\eta}} \right) + \frac{D_T}{T_0}\left(\left(\frac{\partial T}{\partial \tilde{\xi}}\right)^2 + \left(\frac{\partial T}{\partial \tilde{\eta}}\right)^2 \right) \right\}, \tag{3.5}$$

$$\left(\frac{\partial}{\partial \tilde{t}} + \tilde{u}\frac{\partial}{\partial \tilde{\xi}} + \tilde{v}\frac{\partial}{\partial \tilde{\eta}} \right)F = D_B\left(\frac{\partial^2 F}{\partial \tilde{\xi}^2} + \frac{\partial^2 F}{\partial \tilde{\eta}^2} \right) + \frac{D_T}{T_0}\left(\frac{\partial^2 T}{\partial \tilde{\xi}^2} + \frac{\partial^2 T}{\partial \tilde{\eta}^2} \right). \tag{3.6}$$

Where ρ_f represents the fluid density, T is temperature , ρ_p nanoparticle mass density, $\tilde{u}$ is the axial velocity, $\tilde{v}$ is the transverse velocity, $\tilde{\eta}$ is the transverse coordinate, $\tilde{p}$ is the pressure, μ is the fluid viscosity, g is the acceleration due to gravity, β is the volumetric Expansion coefficient of the fluid, $(\rho c)_f$ represents the heat capacity of fluid, $(\rho c)_p$ is the effective heat capacity of nanoparticle, k is the thermal conductivity, F is the nanoparticle volume fraction, D_B is the Brownian diffusion coefficient, D_T is the thermophoretic diffusion coefficient, and ρ_{f0} is the nanofluid density at the reference temperature (T_0). We then present the subsequent non-dimensional parameters

$$\left. \begin{aligned} &\xi = \frac{\tilde{\xi}}{\lambda}, \eta = \frac{\tilde{\eta}}{a}, t = \frac{c\tilde{t}}{\lambda} \quad u = \frac{\tilde{u}}{c}, v = \frac{\tilde{v}}{c\delta}, \quad p = \frac{\tilde{p}a^2}{\mu c\lambda} \\[2mm] &\delta = \frac{a}{\lambda}, h = \frac{\tilde{h}}{a} = 1 + \phi\sin(2\pi\xi), \phi = \frac{b}{a}, v = \frac{\mu}{\rho_{f0}}, \theta = \frac{T-T_0}{T_1-T_0} \\[2mm] &\Phi = \frac{F-F_o}{F_1-F_0}, \mathrm{Re} = \frac{\rho_f ca}{\mu}, Gr_T = \frac{\beta g a^3(1-F_0)(T_1-T_0)}{v^2} \\[2mm] &Gr_f = \frac{\beta g a^3(\rho_p-\rho_{f0})(F_1-F_0)}{v^2\rho_{f0}}, \mathrm{Pr} = \frac{v(\rho c)_f}{k}, \\[2mm] &N_b = \frac{(\rho c)_p D_B(F_1-F_0)}{k}, N_t = \frac{(\rho c)_p D_T(T_1-T_0)}{kT_0}, \end{aligned} \right\} \tag{3.7}$$

where η is non-dimensional axial coordinate, g is non-dimensional transverse coordinate, t is dimensionless time, u and v are non-dimensional axial and transverse velocity components, p is dimensionless pressure, h is transverse vibration of the wall, δ is wave number, Φ is rescaled nanoparticle volume fraction, N_t represents thermophoresis parameter, ϕ represents the amplitude ratio, v represents the nanofluid kinematic viscosity, θ is dimensionless temperature, Re is Reynold number, Gr_T is thermal Grashof number, Gr_F represents the basic-density Grashof number, N_b is the Brownian motion parameter, Pr represents the Prandtl number, k is Nano fluid thermal conductivity.

The Reynold number Re $\rightarrow$ 0 and $\delta \rightarrow$ 0 because of the long wavelength approximation. At the same time $\delta \rightarrow$ 0 cuts out the curvature impacts. Whereas Re $\rightarrow$ 0 represses the inertial forces. As a result of these approximations Eqs. (3.2) to (3.6) become:

$$\frac{\partial u}{\partial \xi} + \frac{\partial v}{\partial \eta} = 0 \quad , \tag{3.8}$$

$$\frac{\partial p}{\partial \xi} = \frac{\partial^2 u}{\partial \eta^2} + Gr_T \theta - Gr_F \Phi , \tag{3.9}$$

$$\frac{\partial p}{\partial \eta} = 0, \tag{3.10}$$

$$\frac{\partial^2 \theta}{\partial \eta^2} + N_b \frac{\partial \theta}{\partial \eta} \frac{\partial \Phi}{\partial \eta} + N_t \left(\frac{\partial \theta}{\partial \eta} \right)^2 = 0, \tag{3.11}$$

$$\frac{\partial^2 \Phi}{\partial \eta^2} + \frac{N_t}{N_b} \frac{\partial^2 \theta}{\partial \eta^2} = 0. \tag{3.12}$$

The thermal and hydronamic boundary conditions which are cited in Refs: [1, 29 ,30] , are given as follows.

$$\theta\big|_{\eta=0}=0, \qquad \theta\big|_{\eta=h}=1, \quad \Phi\big|_{\eta=0}=0, \quad \Phi\big|_{\eta=h}=1, \quad \frac{\partial u}{\partial \eta}\bigg|_{\eta=0}=0, \qquad u\big|_{\eta=h}=0. \quad (3.13)$$

Integrate Eq. (3.12) two times with respect to η and apply the first, second, third and fourth boundary conditions, we acquire the nanoparticle fraction field as:

$$\Phi=-\frac{N_t}{N_b}e^{n(h-n)}\left(\frac{e^{n\eta}-1}{e^{nh}-1}\right)+\frac{n}{N_b}\eta , \qquad (3.14)$$

Where, $n=\dfrac{Nt+Nb}{h}$. To find the temperature field, put the Eq. (3.14) into Eq. (3.11) and integrate Eq. (3.11) two times with respect to η and then apply the second and fourth boundary conditions of Eq. (3.13).

$$\theta=e^{n(h-n)}\left(\frac{e^{n\eta}-1}{e^{nh}-1}\right). \qquad (3.15)$$

To find the axial velocity, replace the values of Φ and θ in Eq. (3.9) and double integrate it with respect to η and then apply the fifth and sixth boundary conditions of Eq. (3.13).

$$u=-\frac{1}{2}\frac{dp}{d\xi}(\eta^2-h^2)+m\left\{\frac{1}{n^2}(e^{-n\eta}-e^{-nh})-\frac{1}{2}(\eta^2-h^2)\right\}+\frac{nGr_F}{6N_b}(\eta^3-h^3)+\frac{m}{n}(\eta-h), \qquad (3.16)$$

Where, $m=\left(Gr_T+\dfrac{N_t}{N_b}Gr_F\right)\left(\dfrac{e^{nh}}{e^{nh}-1}\right).$

The volume flow rate is defined as follows [28]

$$Q=\int_0^h u\,d\eta . \qquad (3.17)$$

The following equation is obtained by using Eq. (3.16) into Eq. (3.17).

11

$$Q = -\frac{h^3}{3}\frac{dp}{d\xi} + m\left\{\frac{1}{n^2}\left(\frac{1}{n} - \frac{\frac{1}{n}+h}{e^{nh}}\right) - \frac{h^2}{2n} + \frac{h^3}{3}\right\} + \frac{nGr_F}{8N_b}h^4 \quad . \tag{3.18}$$

The wave frame ($\tilde{X}$, $\tilde{Y}$) is going with the velocity c, the transformation among a wave frame ($\tilde{X}$, $\tilde{Y}$) and the fixed frame ($\tilde{\xi}, \tilde{\eta}$) are considered as cited in Refs: [32-37]:

$$\tilde{X} = \tilde{\xi} - c\tilde{t}, \tilde{Y} = \tilde{\eta}, \tilde{U} = \tilde{u} - c, \tilde{V} = \tilde{v} \tag{3.19}$$

Where ($\tilde{U}$, $\tilde{V}$) are the velocity components in the wave frame and ($\tilde{u}$, $\tilde{v}$) are the velocity components in the fixed frame respectively. The volume flow rate in wave frame can be calculated with the following relation:

$$Q = \int_0^h (U+1)dY \ , \tag{3.20}$$

We integrate it and get the following expression:

$$Q = q + h \ , \tag{3.21}$$

And $q = \int_0^h U dY$.

By taking the average of volume flow rate through one time period, we have:

$$\bar{Q} = \int_0^1 Q dt = \int_0^1 (q+h)dt . \tag{3.22}$$

From Eq. (3.21) and Eq. (3.22), we reach to following equation:

$$\bar{Q} = Q + 1 - h = q + 1 . \tag{3.23}$$

Eq. (3.18) and Eq. (3.23) produce a compressed form for the pressure gradient:

$$\frac{dp}{d\xi} = -\frac{3}{h^3}(\bar{Q}-1+h) + m\left\{\frac{3}{n^2h^3}\left(\frac{1}{n} - \frac{\frac{1}{n}+h}{e^{nh}}\right) - \frac{3}{2nh} + 1\right\} + \frac{3hnGr_F}{8N_b} \quad . \tag{3.24}$$

The pressure difference over one wavelength (Δp) is:

$$\Delta p = \int_0^1 \frac{dp}{d\xi} d\xi,$$ (3.25)

From Eq. (3.16) and applying the transformations of Eq. (3.19), the stream function in the wave frame (obeying the Cauchy–Riemann equations $U = \frac{\partial \psi}{\partial \eta}, V = -\frac{\partial \psi}{\partial \xi}$) becomes:

$$\psi(\xi,\eta) = \frac{1}{2}\frac{dp}{d\xi}\left(\frac{\eta^3}{3} - h^2\eta\right) + m\left\{\frac{1}{n^2}\left(-\frac{e^{-n\eta}}{n} - e^{-nh}\eta + \frac{1}{n}\right) - \frac{1}{2}\left(\frac{\eta^3}{3} - h^2\eta\right) + \frac{1}{n}\left(\frac{\eta^2}{3} - h\eta\right)\right\} + \frac{nGr_F}{6N_b}\left(\frac{\eta^4}{4} - h^3\eta\right) - \eta$$ (3.26)

3.2 Numerical Results and Discussion:

The peristaltic fluid regime's geometry is demonstrated in the figure 2. The impact of Nano fluid features on the peristaltic flow pattern is studied graphically.

All explanations have been produced by using Mathematica software. The impacts of Brownian motion parameter N_b and also the impacts of thermophoresis parameter N_t on Nanoparticle fraction profile and temperature profile are depicted in Figs. 3.2 and 3.3.
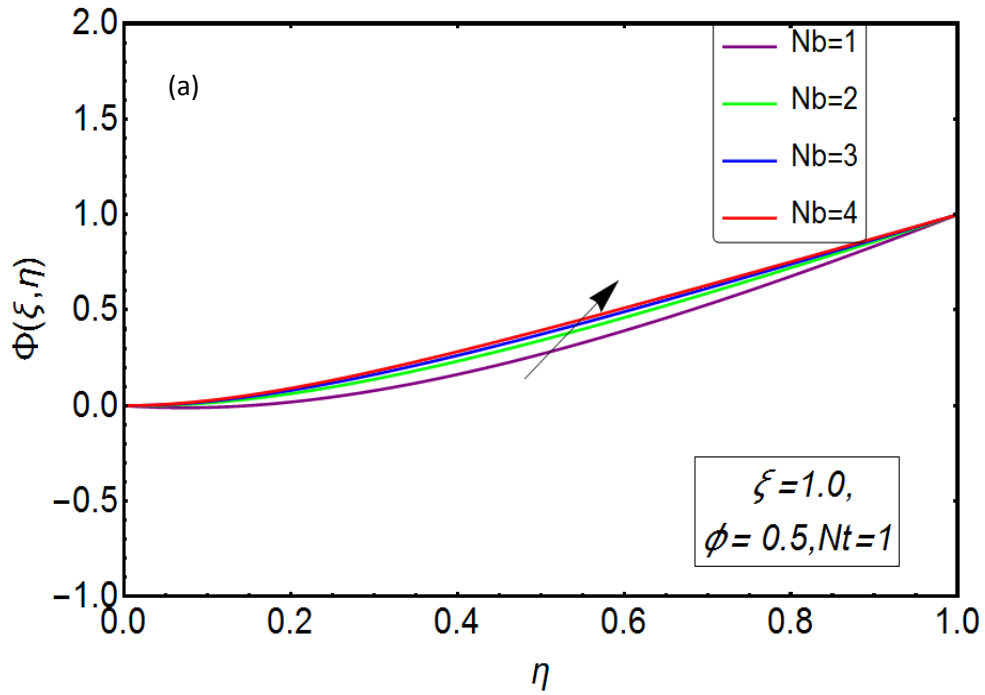
Fig. 3.2(a) Nanoparticle fraction profiles $\Phi(\xi,\eta)$ (η) at ϕ =0.5, ξ=1.0 for N_t =1.0, N_b=1,2,3,4
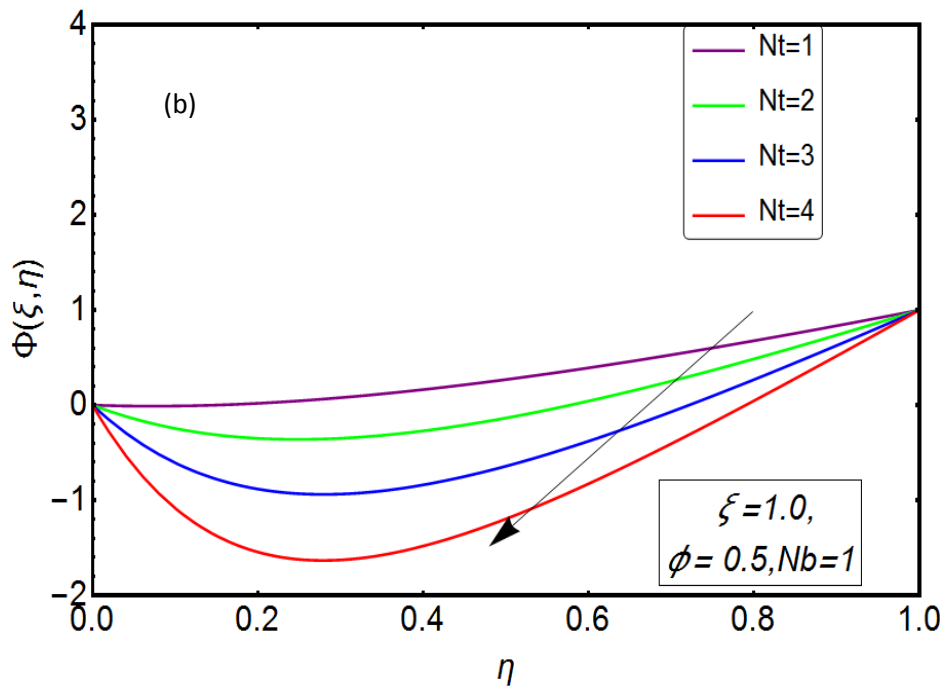
Fig. 3.2(b) Nanoparticle fraction profiles $\Phi(\xi,\eta)$ at ϕ =0.5, ξ =1.0 for N_b=1, N_t =1,2,3,4.
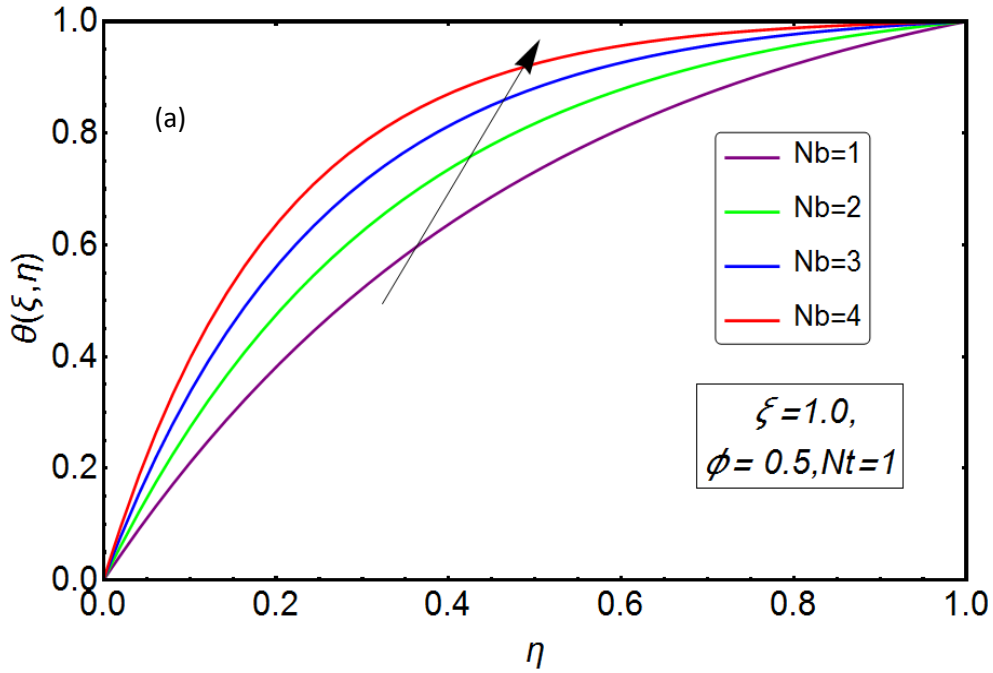
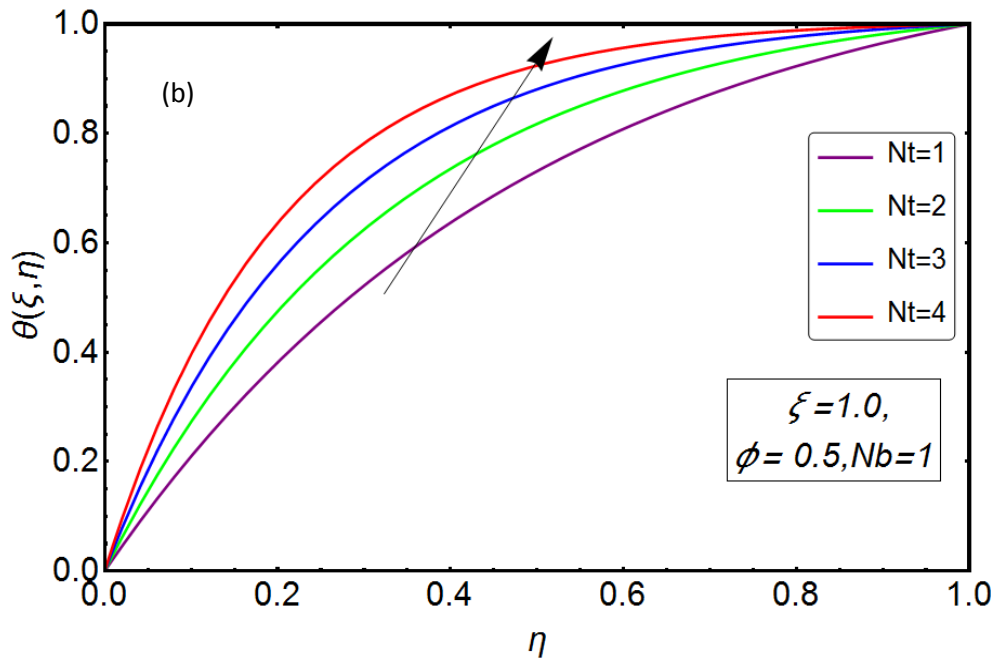Fig. 3.3(b) Temperature profile $\theta(\xi,\eta)$ at ϕ =0.5, ξ =1.0 for N_b=1, N_t =1,2,3,4.

Fig. 3.3(a) Temperature profile $\theta(\xi,\eta)$ at ϕ =0.5, ξ =1.0 for (a) N_t =1.0, N_b=1,2,3,4

Brownian motion parameter N_b emerges in the energy and species conservation equations. Definitely Brownian motion parameter N_b is a significant parameter thus in impacting the species

15

diffusion. Fig. 3.2a shows the effect of Brownian motion parameter N_b, by increasing the values of Brownian motion parameter N_b the nanoparticle fraction profile is increased. The Nano fluid acts similar to a fluid as compare to the solid-fluid mixtures in which comparatively huge particles with millimeter and micrometer orders are dangled. Nano fluid is basically two-phase fluid and unspecified motion of the dangled nanoparticles increases the energy interchange rate but in the meanwhile oppresses the concentration in the flow regime. We observe that for the larger values of the dimensionless transverse coordinate there is a clear divergence in profiles. For example, as we relocate from the channel center line the profiles move aside. This movement has been noticed by Akbar and Nadeem [25]. With an increase in the value of N_t from 0 to 4 there is a noticeable decrease in $\Phi(\eta)$. Just like Brownian motion parameter N_t emerges in energy as well as nanoparticle volume concentration conservation equations (3.11) and (3.12). Thus species diffusion is highlighted with thermophoresis. The pattern is unchanged with macroscopic convection flows as displayed by Zueco J [26]. Same results have been acquired in Nano fluid studied by Kuznestov and Nield [27].

Figs.3.3 (a) and 3.3(b) show that N_t and N_b have same effects on temperature distributions for some transverse distance from the center of the channel. At the start $\theta(\eta)$ is increased with an increase in N_t and N_b. Thermophoresis is the phenomenon in which nanoparticles move towards decreasing temperature gradient. Clearly this phenomenon has vigorous impact on temperature evolution.
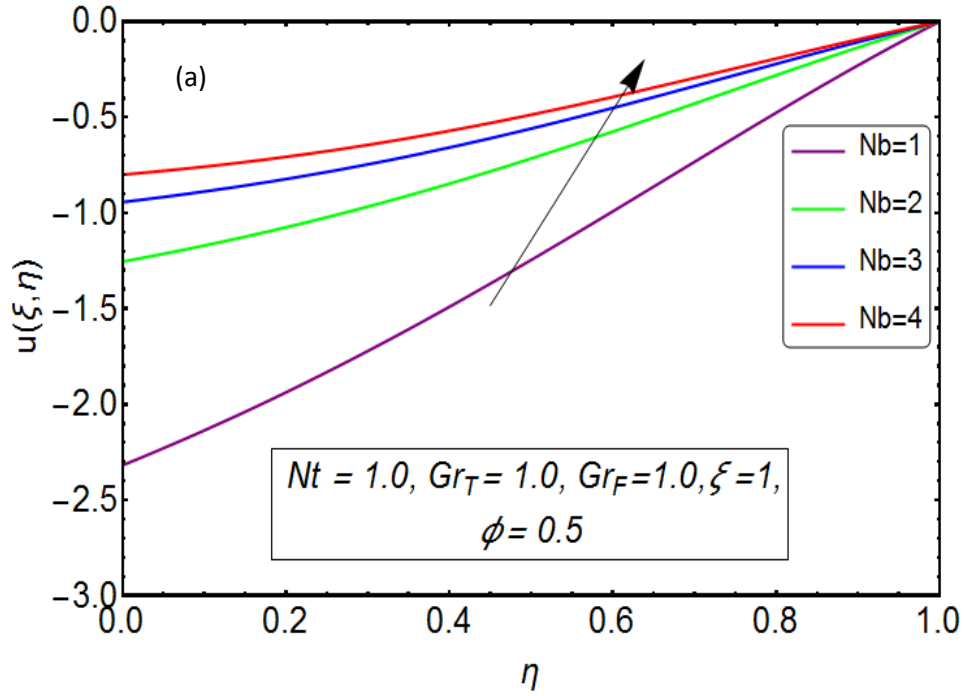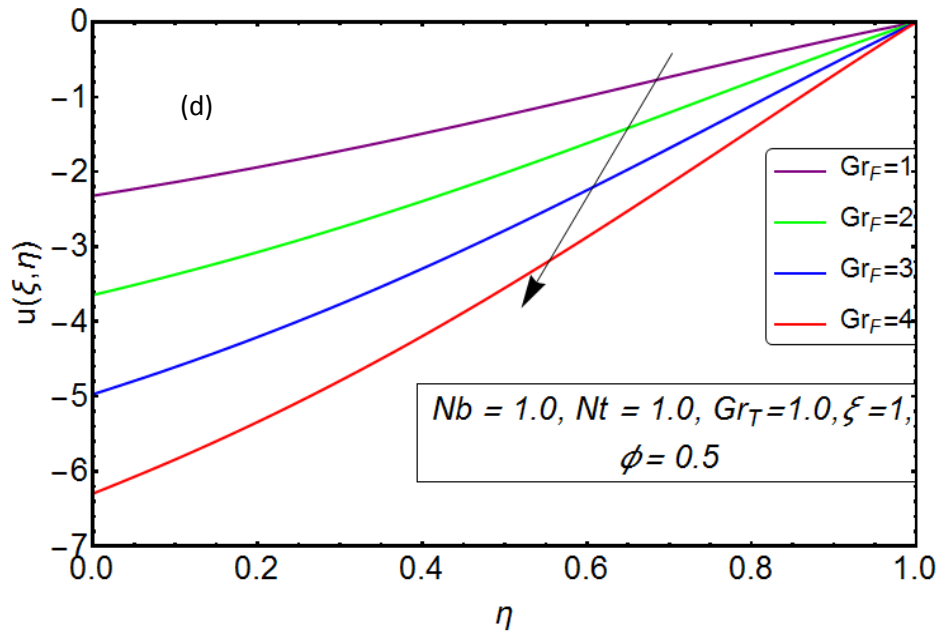
Figs. 3.4.(a) Velocity profile $u(\xi, \eta)$ at ϕ =0.5, ξ =1.0 for N_t =1, Gr_T=1, Gr_F=1, N_b=1,2,3,4
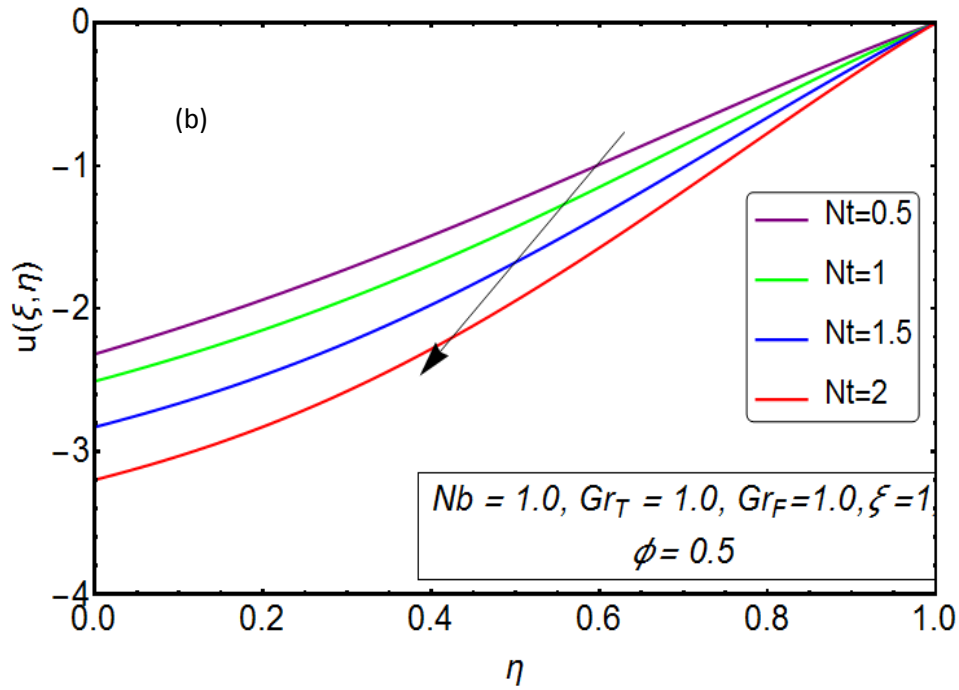
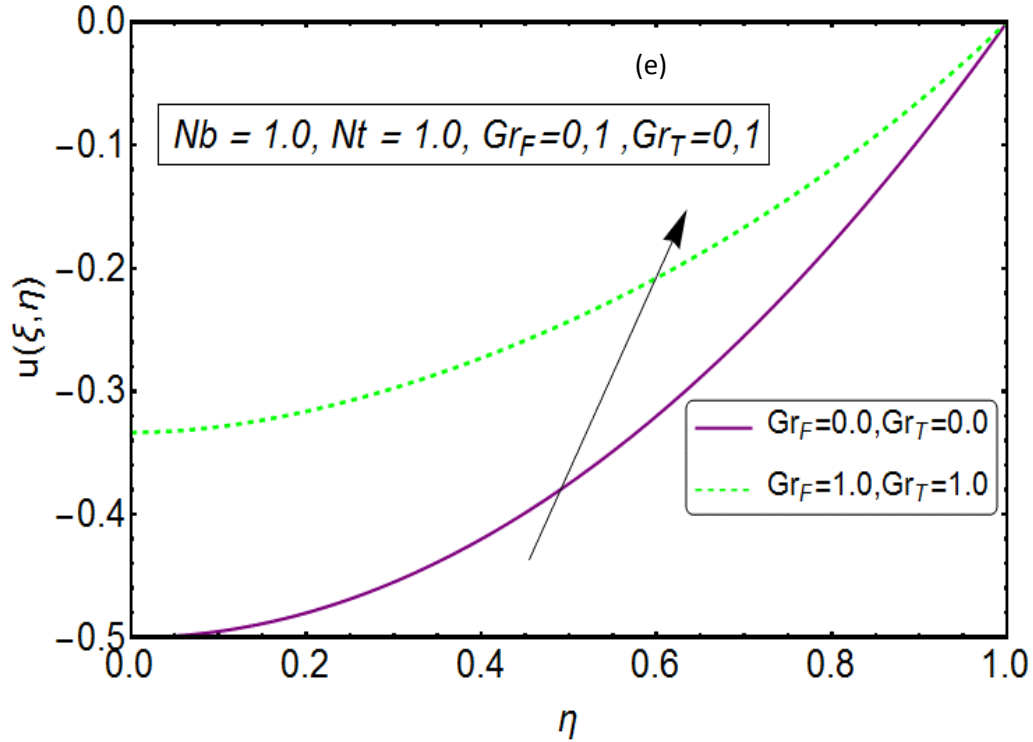Figs. 3.4.(b) Velocity profile $u(\xi, \eta)$ at ϕ =0.5, ξ =1.0 for N_b=1, Gr_T=1, Gr_F=1, N_t =0.5,1,1.5,2
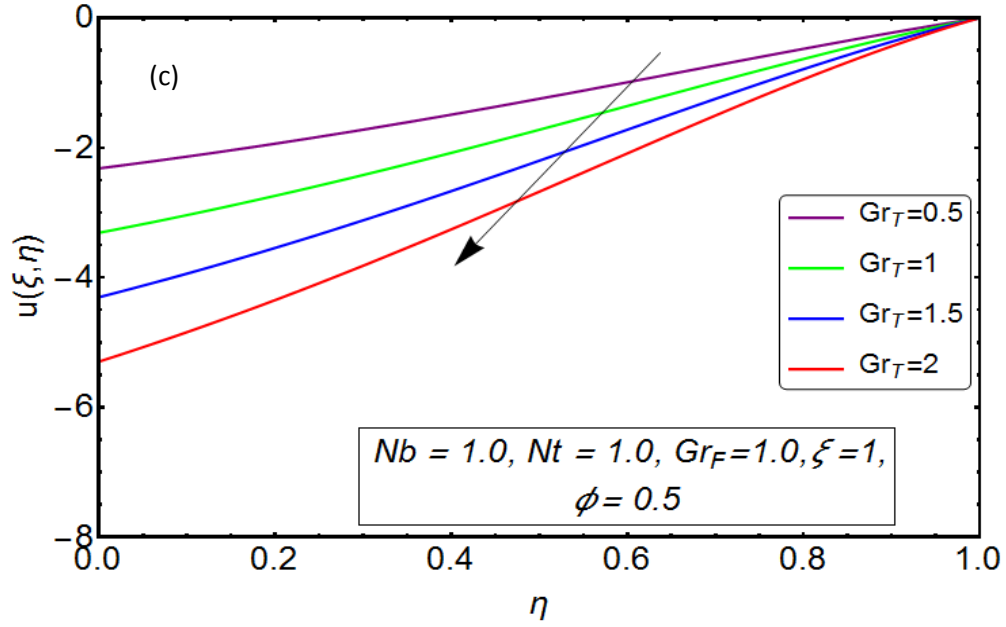
Figs. 3.4.(c) Velocity profile $u(\xi,\eta)$ at ϕ =0.5, ξ =1.0 for (c) N_t =1, Gr_F=1, N_b=1, Gr_T=0.5,1,1.5,2

Figs.3.4.(d) Velocity profile $u(\xi,\eta)$ at ϕ =0.5, ξ =1.0 for N_t =1, N_b=1, Gr_T=1, Gr_F=1,2,3,4.

Figs.3.4.(e) Velocity profile $u(\xi,\eta)$ at ϕ =0.5 ξ ,=1.0 for N_b=1, N_t =1, Gr_T=0,1, Gr_F=0,1 .

Figs.3.4(a)-(e)exhibit that for the channel half space the axial velocity is negative therfore reverse flow occurs. Velocities are maximum at the centre of the channel and reaches to zero at the wall of the channel.

Fig. 3.4(a) shows that the magnitude of the velocity decreases with an increase in values of N_b from 1 to 4.

Fig. 3.4(b) indicates that with an icrease in the values of Brownian motion parameter Nt from 0.5 to 1 to 1.5 to 2, the magnitude of the axial velocity increases.

Fig. 3.4(c) Indicates the impact of thermal grashof number Gr_T on axial velocity.Grt indicates the relative impact of viscous hydronamic force and thermal buyoncy force.For Gr_T >1 the peristaltic reigon is governed by buyoncy forces. For Gr_T <1 peristatic reigon is governed by viscous forces. And for the case where Gr_T is equal to the value 1, thermal buyoncy forces and viscous forces having same magnitude as explained by Beg et al.[38]. The immensity of the axial velocity increases with an increase in the values of Gr_T . The monotonic pattern is observed for 0.5≤ Gr_T

≤ 1.5. But for Gr_T =2, the profile which is noticed has a wavy form the centre of the channel to the wall of the channel. Fig. 3.4(c) indicates that magnitude of the velocity increases with an increase in the values of Gr_T.

Fig. 3.4(d) indicates that magnitude of the axial velocity increases with an increase in basic density grashof number Gr_F i.e. it aggravates the reversal flow reverse flow in the domain.

Gr_F is the ratio of species buyoncy force to viscous hydronamic force. Axial velocity is lessened at Gr_F =1. In Fig.3.4(e) we have done the comparison between non thermal, Newtonian results of shapiro AH [1] and thermal species buyoncy forces which are equivalent to the viscous force. Nanofluids evidently reveal the reduced reversal flow compared with Newtonian fluids.
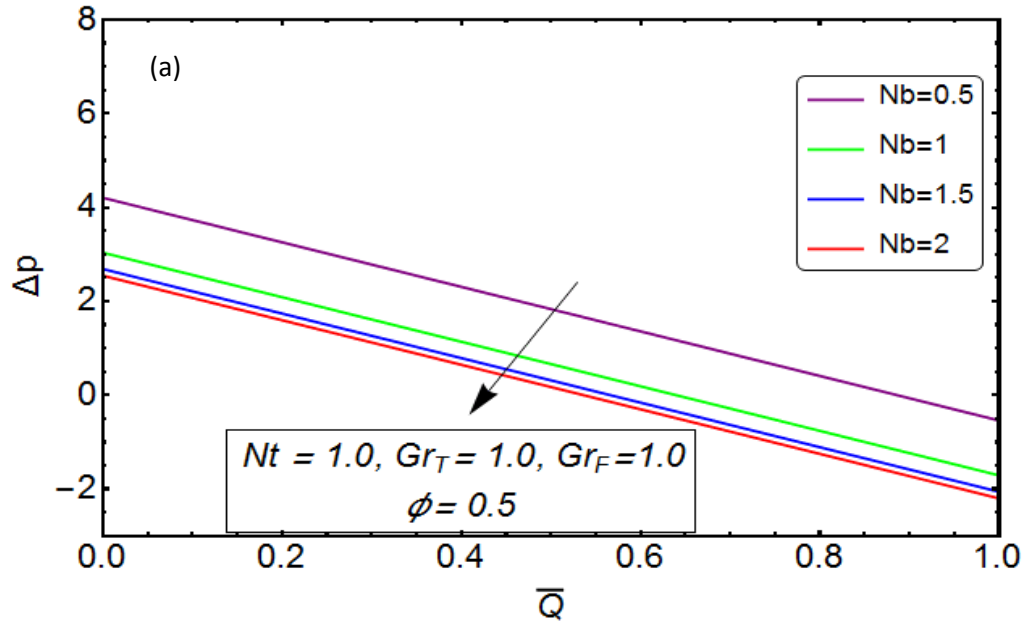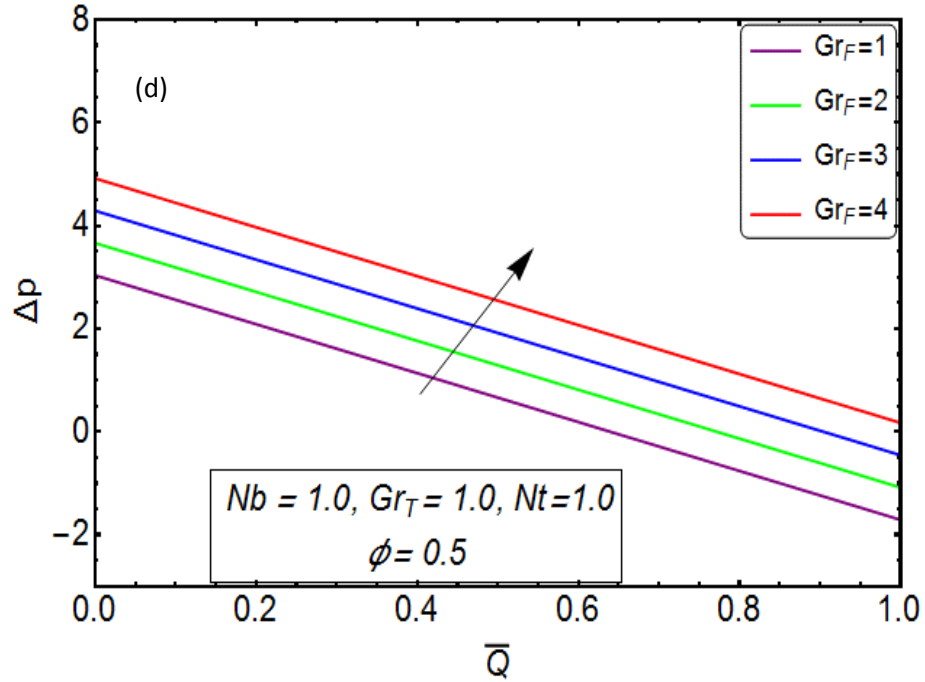

Figs. 3.5.(a) Pressure diffrence across one wavelength (Δp) vs $(\bar{Q})$ at ϕ=0.5 for N_t =1, Gr_T=1, Gr_F=1, N_b=0.5,1,1.5
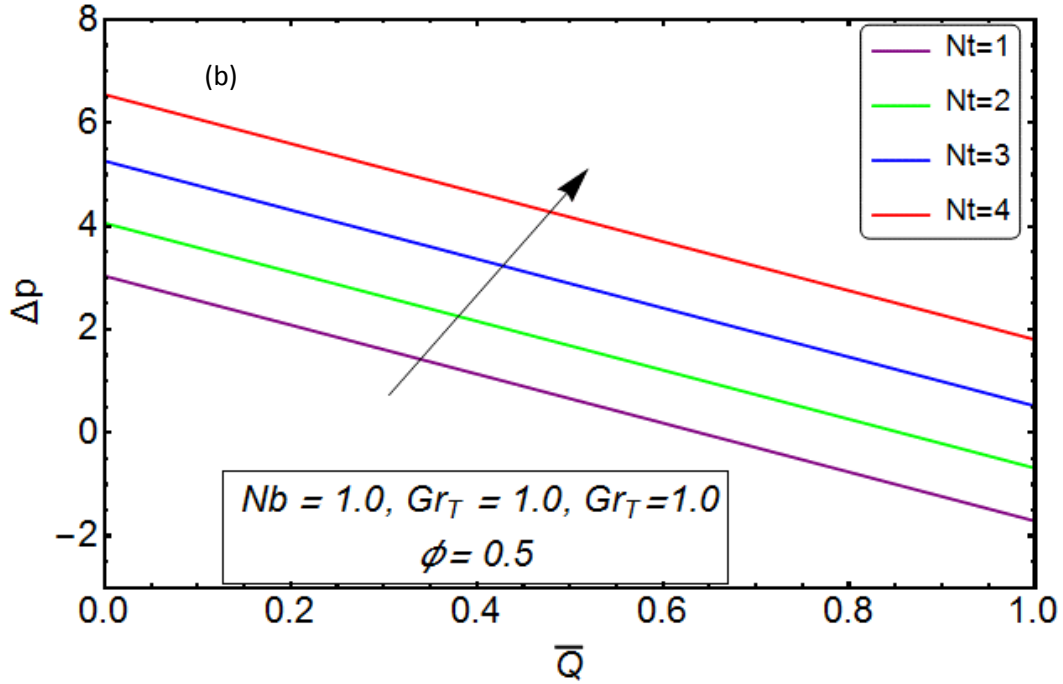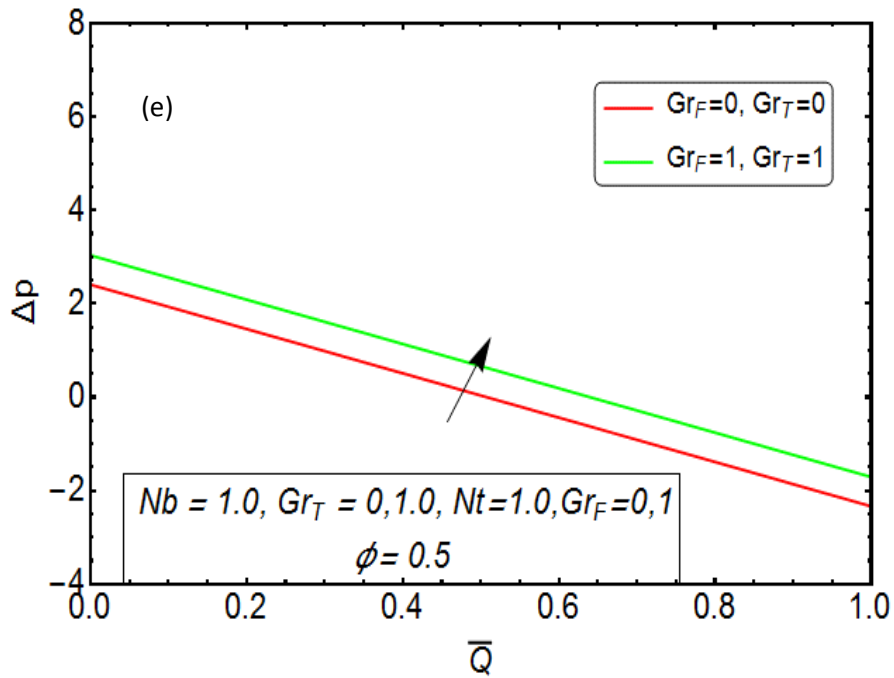
Figs. 3.5. Pressure diffrence across one wavelength (Δp) vs ($\bar{Q}$) at ϕ=0.5 for (b) N_b=1, Gr_T=1, Gr_F=1, N_t =1,2,3,4
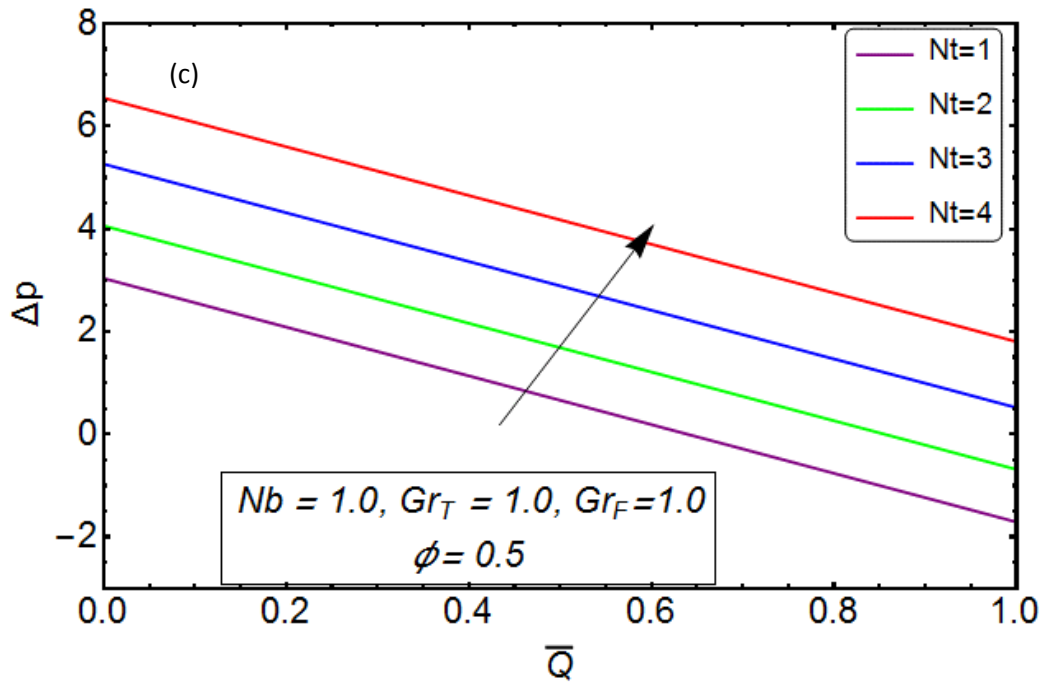
Figs. 3.5.(c) Pressure diffrence across one wavelength (Δp) vs ($\bar{Q}$) at ϕ=0.5 for N_t =1, Gr_F=1, N_b =1, Gr_T=0.5,1,1.5,2.

Figs. 3.5.(d) Pressure diffrence across one wavelength (Δp) vs $(\bar{Q})$ at ϕ=0.5 for N_t =1, N_b=1,Gr_T=1, Gr_F=1,2,3.

Figs. 3.5.(e) Pressure diffrence across one wavelength (Δp) vs $(\bar{Q})$ at ϕ=0.5 for N_t =1, N_b=1, Gr_T=0,1, Gr_F=0,1.

Figs. 3.5(a)-(e) represents the impacts of Brownian motion parameter N_b, thermal Grashof number Gr_T, thermophoresis parameter N_t and basic-density Grashof number Gr_F on pressure difference over one wave length. In each time linear distributions are noticed. Akbar and Nadeem got the same trend however they used the homotopic perturbation method.

Δp >0, Δp =0, Δp <0 are three ranges of pumping. We are interested in dealing with first two ranges because they are more applicable in medial engineering.

Fig. 3.5(a) shows that there is a decrease in pressure difference with an increase in Brownian motion parameter N_b.

Fig. 3.5(b) shows that pressure difference strongly increases with an increase in Thermophoresis Parameter N_t. Therefore in Nano-peristaltic pumps, pressure difference can be simply maintained by increasing the Brownian motion effect and thermophoretic effect for all functioning flow rates.

Fig. 3.5(c) shows that the pressure difference increases rapidly with an increase in Gr_T for all flow rates.

Fig. 3.5(d) illustrates that pressure difference increases with an increase in Gr_F for all flow rates. In Fig. 3.5(e) we compared the Nano fluids with Newtonian fluids. Nano fluids present a fundamental increase in pressure difference that is why they are more suitable in practical peristaltic pumps.
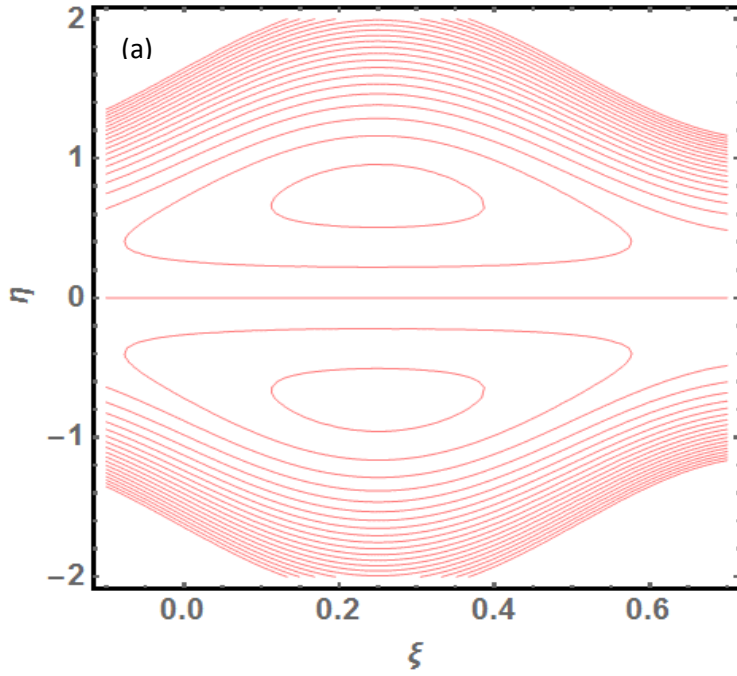
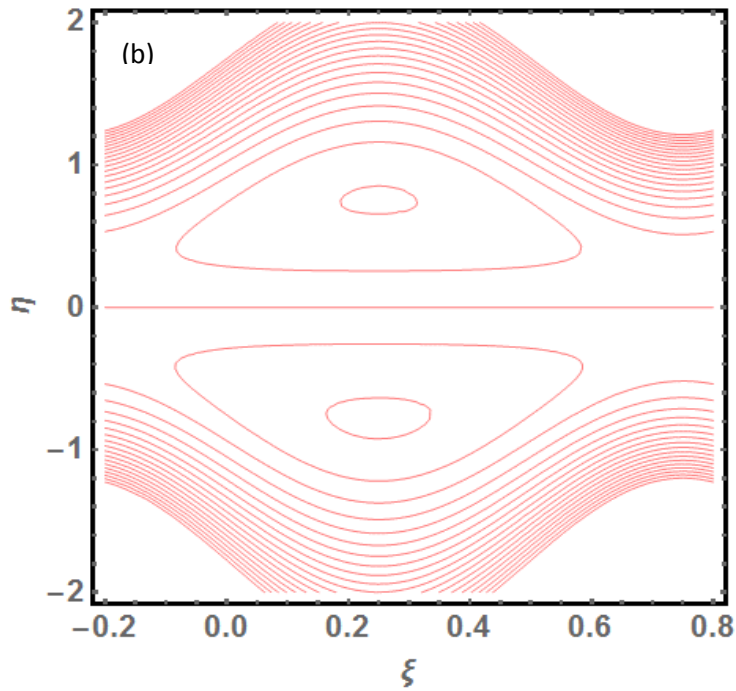Fig. 3.6.(a) Stream lines at $\bar{Q}$ =0.9, ϕ=0.4, N_b=1, N_t =1, Gr_T= 0, Gr_F=0 (Newtonian fluids)

Fig. 3.6. (b) Stream lines at ($\bar{Q}$) =0.9, ϕ=0.4, N_b=1, N_t =1, Gr_T=0.1, Gr_F=0.01.

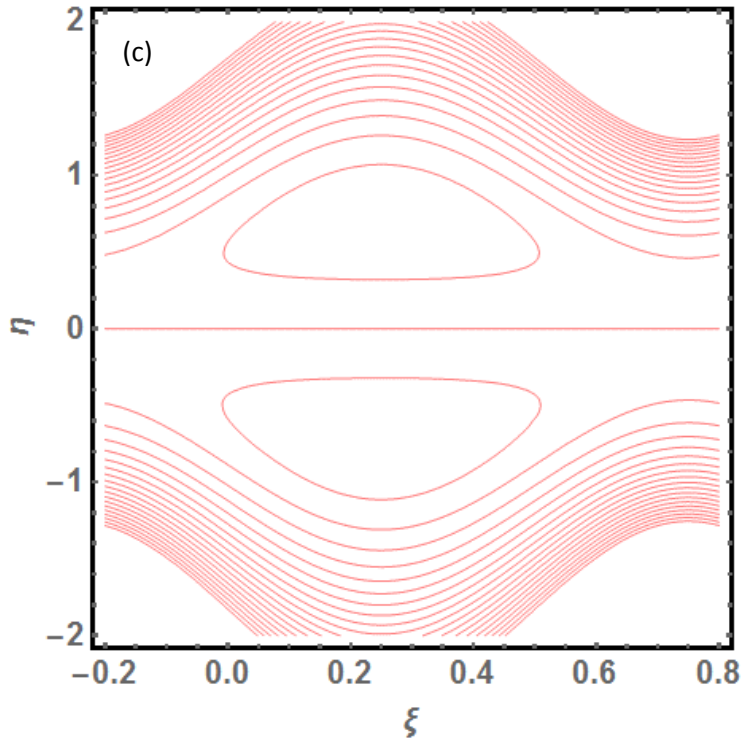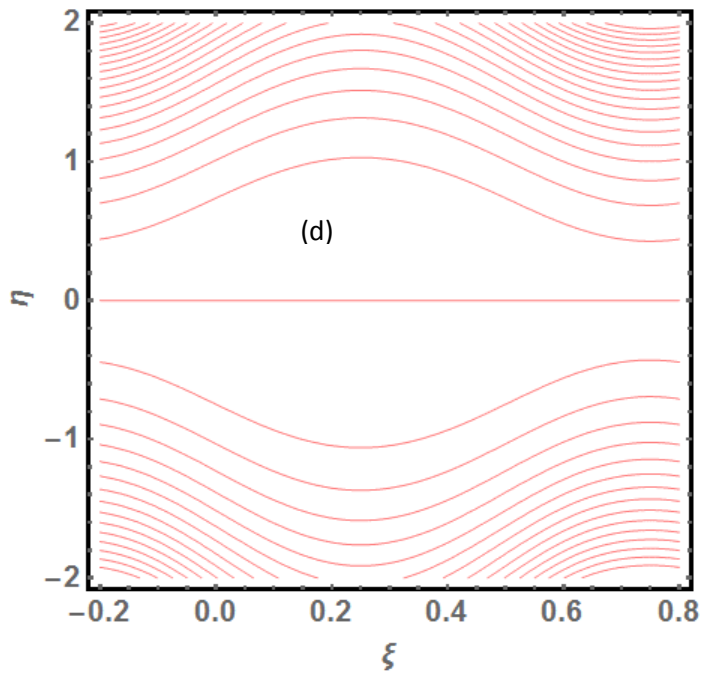Fig. 3.6.(c) Stream lines at $\bar{Q}$ =0.9, ϕ=0.4, N_b=0.5, N_t =1, Gr_T=0.1, Gr_F=0.01

Figs. 3.6.(d)Stream lines at $\bar{Q}$ =0.9, ϕ=0.3, N_b=1, N_t =0.5, Gr_T=0.1, Gr_F=0.01.

Fig. 3.6.(e) Stream lines at $\overline{Q}$ =0.9, ϕ=0.4, N_b=0.5, N_t =1, Gr_T=0.1, Gr_F=0.01 .

Figs. 3.6. (f) Stream lines at $\overline{Q}$ =0.9, ϕ=0.4, N_b=1 N_t =0.1, Gr_T=0.1, Gr_F=0.01.

Figs. 3.6.(g) Stream lines at $\bar{Q}$ =0.9, ϕ=0.4, N_b=1, N_t =1, Gr_T=0.05, Gr_F=0.01.
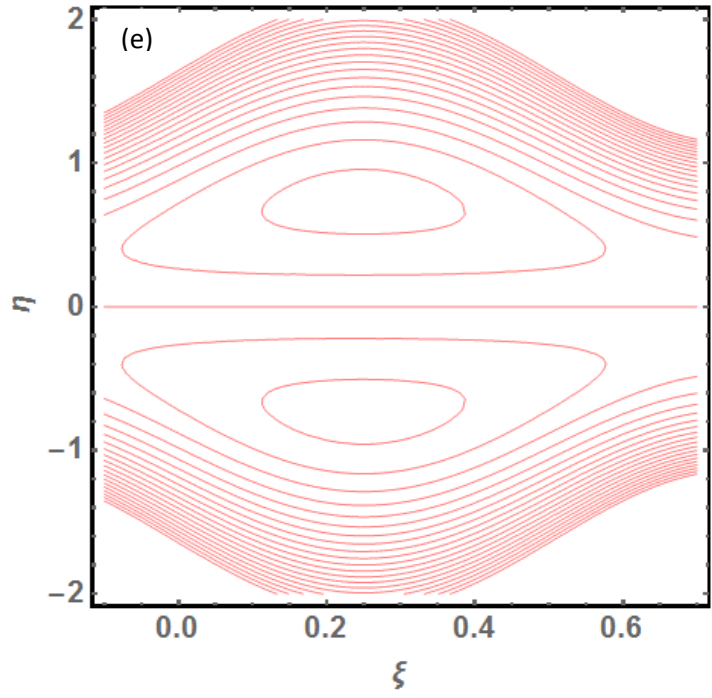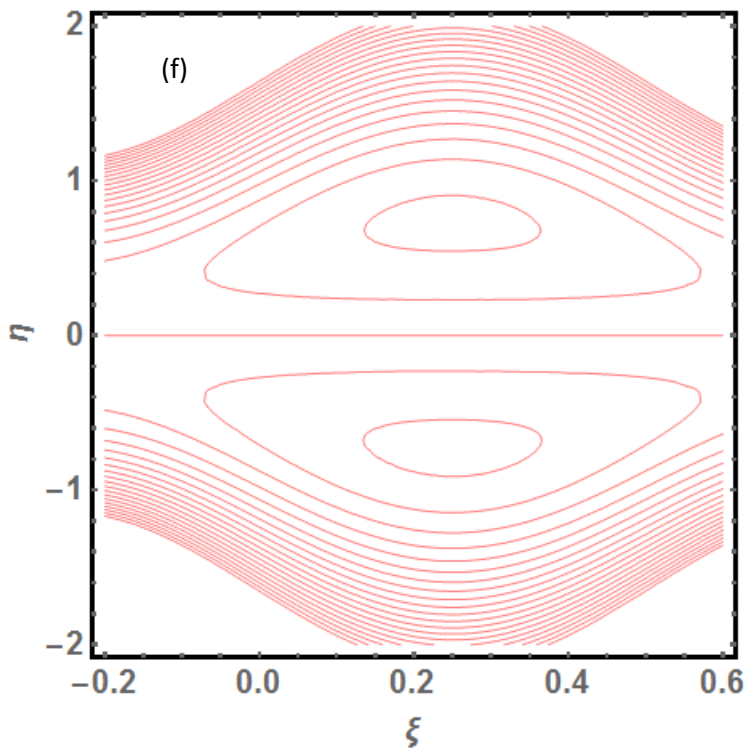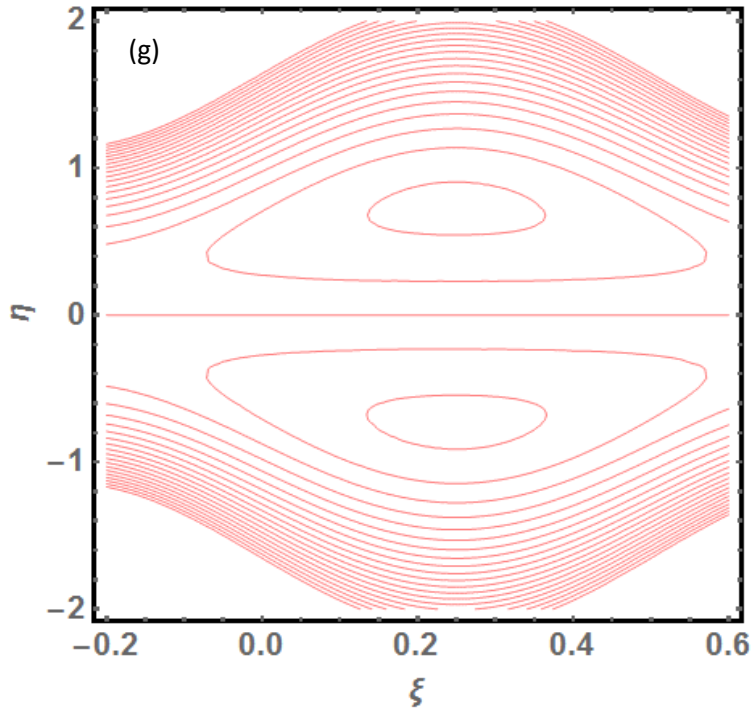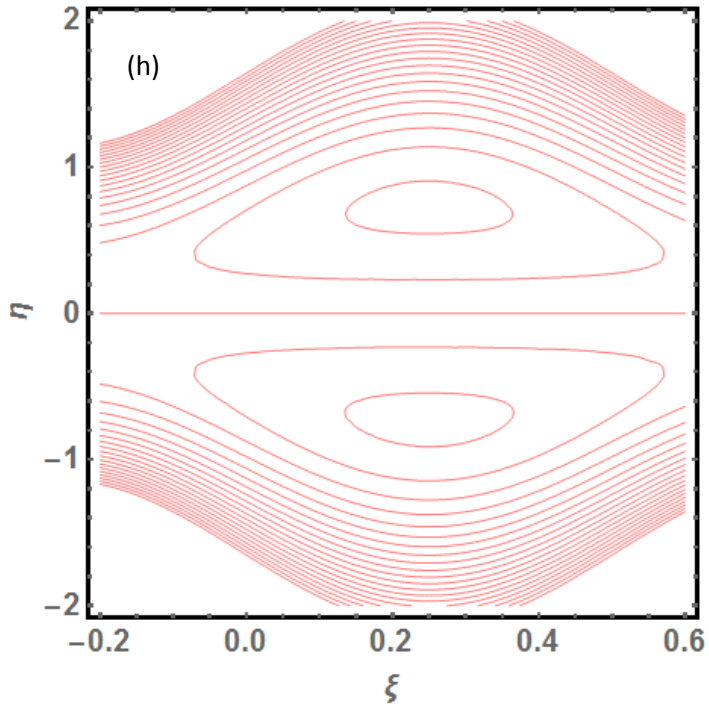

Figs. 3.6. (h) Stream lines at $\bar{Q}$ =0.9, ϕ=0.4, N_b=0.5, N_t =1, Gr_T=0.01, Gr_F=0.01.
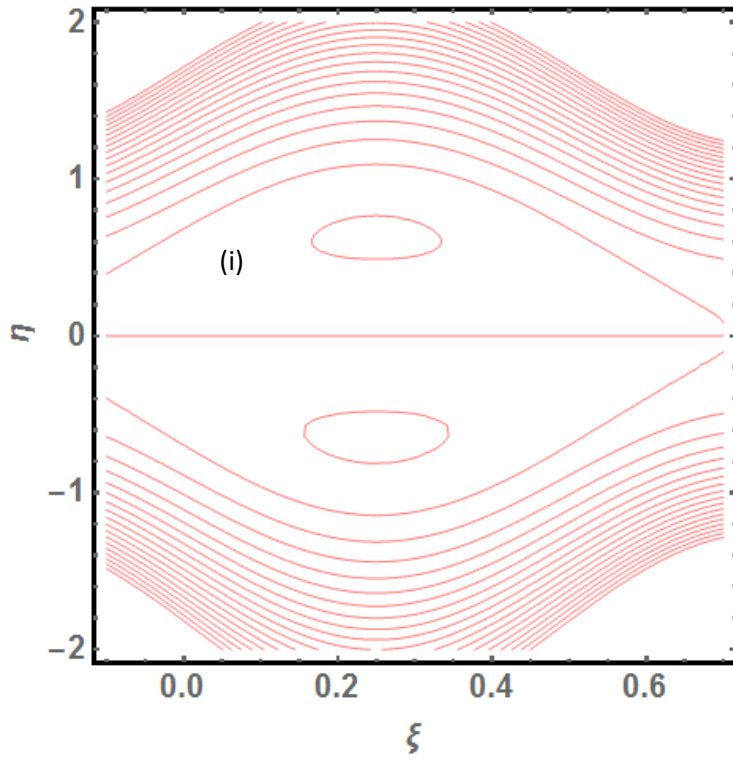
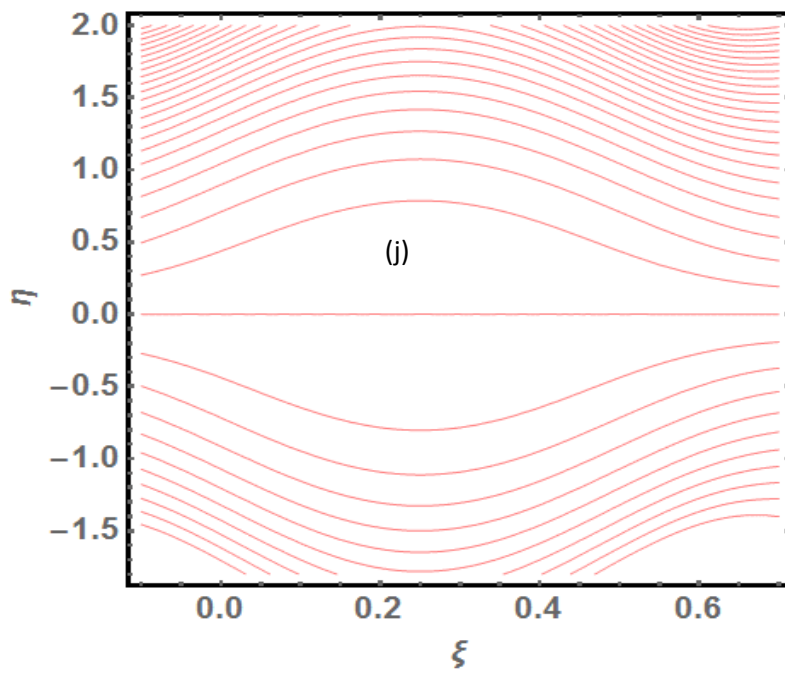Fig. 3.6.(i) Stream lines at $\bar{Q}$ =0.8, ϕ=0.4, N_b=1, N_t =1, Gr_T=0.1, Gr_F=0.02.

Fig. 3.6. (j) Stream lines at $\bar{Q}$ =0.5, ϕ=0.4, N_b=1, N_t =1, Gr_T=0.1, Gr_F=0.03

From Fig. 3.6(a)-(j) ten streamline distributions are shown, the impacts of Brownian motion parameter N_b, thermal Grashof number Gr_T, thermophoresis parameter N_t and basic-density Grashof number Gr_F on trapping are represented. In each case ф and the average volume flow rate $\bar{Q}$ are fixed at 0.5 and 0.6 respectively. Only one parameter is changed for each pair. The streamlines are categorized under particular conditions to encircle the bolus of fluid particles called trapping, which is the feature of peristaltic motion as explained by Fung and Yih [28]. The bolus has the same speed as that of the wave as it is trapped by the wave.

Comparing Fig. 3.6(a) and 3.6(b), we have increased the values of thermal Grashof number from 0.0 to 0.1 and basic density Grashof number from 0.0 to 0.01 the magnitude of the trapped bolus is reduced.

Comparing 3.6(c) and 3.6(d), by decreasing the value of Brownian motion parameter N_b from 0.5 to 0.1 the dual bolus is reduced to the single bolus.

Comparing 3.6(e) and 3.6(f), with decreasing the value of thermophoresis parameter from 0.5 to 0.1 the magnitude of the bolus is increased.

Comparing 3.6(g) and 3.6(h), the bolus size is magnified when thermal Grashof number is decreased from the value 0.05 to 0.01.

Comparing 3.6(h) and 3.6(i), species Grashof number is increased from the value 0.02 to 0.03, the dual bolus is contracted to single bolus. This shows that Nano fluids features therefore unquestionably apply a meaningful effect on peristaltic flow patterns.

Conclusions:

The effects of nanofluid features on peristaltic heat transfer in a two dimensional have been observed by using Mathematica. Numerical computations have shown that:

1. $\Phi(\xi,\eta)$ increases by increasing the values of N_b. Also $\Phi(\xi,\eta)$ decreases by increasing the values of N_t.

2. $\theta(\xi,\eta)$ increases with an increase in N_b and N_t.

3. The magnitude of axial velocity reduces by increasing the values of N_b.

4. The magnitude of axial velocity increases with the increase in the values of Gr_T.

5. The pressure difference is reduced by increasing N_b. The pressure difference increases by increasing the values of N_t.

6. The pressure difference increases by increasing the values of Gr_T and Gr_F.

7. Size of boluses increases by decreasing values of N_t.

8. Size of boluses increases by decreasing the values of Gr_T.

9. A dual bolus reduces to single bolus by increasing the values of Gr_F.

Chapter 4

Carbon Nanotube Analysis for an Unsteady Physiological Flow in a Non-Uniform Channel of Finite Length.

4.1. Introduction:

An analytical investigation is presented to study the unsteady peristaltic transport of nanofluids. Carbon nanotubes analysis is taken into account. To investigate our model for broad scale of biomedical applications, the flow geometry is taken as non-uniform channel of finite length. For the non-dimensional governing equations subject to physically realistic boundary conditions, exact solutions are acquired. With the help of graphical illustrations, the impacts of carbon nanotubes on effective thermal conductivity, axial velocity, transverse velocity, temperature, and pressure difference distributions along the length of non-uniform channel by varying different flow parameters are studied. An inherent characteristic of peristaltic transport i.e. trapping is also studied. We have noticed that MWCnt's have this exceptional quality to increase the axial velocity as well as the transverse velocity of the governing fluids.This model is applicable in drugs delivery system where different geometries of drugs are delivered and it is also applicable to design a micro peristaltic pump for transportation of Nano-fluids.

4.2. Mathematical Formulation:

The geometric model for the peristaltic transport of nanofluid with different nanoparticles via a non-uniform finite length channel, as depicted in Fig.4.1 is taken as:

$$\tilde{h}(\tilde{\zeta}, \tilde{t}) = a(\tilde{\zeta}) - b \cos \frac{\pi}{\lambda} (\tilde{\zeta} - c\tilde{t}), \tag{4.1}$$

where $a(\tilde{\zeta}) = a_0 + \alpha\,\tilde{\zeta}$, is the half width of the channel at any axial distance $\tilde{\zeta}$ from inlet and a_0 , $b, \lambda, \tilde{\zeta}, c, \tilde{t}$ are the half width at the inlet, amplitude, wavelength, axial coordinate, wave velocity and time. α is non-uniformity constant, when $\alpha \to 0$, the non-uniform channel reduces to a uniform channel.
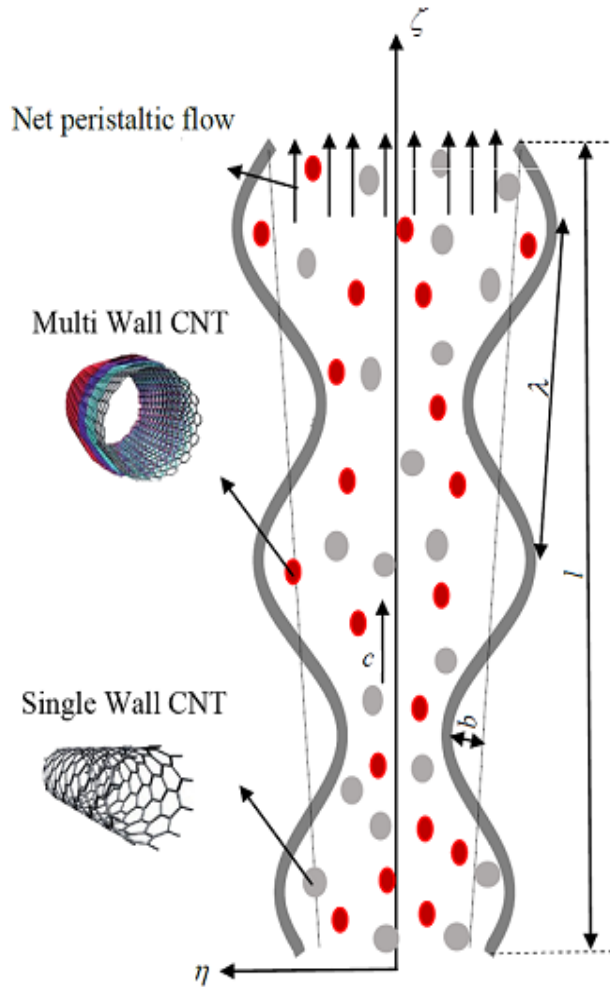

Fig. 4.1: Schematic representation of unsteady peristaltic transport through finite length non-uniform channel.

The peristaltic flow geometry is approximated to a finite length non-uniform channel with sinusoidal waves propagating along the flow direction. The channel walls are supposed to be distensible and identical in constitution. Damping characteristics are ignored. Flow equations will

be modified with low-Reynolds number regime (laminar flows) under long wavelength assumption. The magnitudes for temperature T at the wall of the channel ($\eta = h$) are denoted as T_1. Under the usual Boussinesq approximation, with an appropriate reference pressure, the transport equations in Ref: [40] for the regime are respectively with the following assumptions: (a) laminar incompressible flow, (b) no chemical reactions, (c) negligible external forces, (d) negligible viscous dissipation, (e) negligible radioactive heat transfer, (f) nanoparticles and base fluid locally in thermal equilibrium.

Law of conservation of mass in component form:

$$\frac{\partial \tilde{u}}{\partial \tilde{\zeta}} + \frac{\partial \tilde{v}}{\partial \tilde{\eta}} = 0, \tag{4.2}$$

Axial momentum equation:

$$\rho_{nf}\left(\frac{\partial}{\partial \tilde{t}} + \tilde{u}\frac{\partial}{\partial \tilde{\zeta}} + \tilde{v}\frac{\partial}{\partial \tilde{\eta}}\right)\tilde{u} = -\frac{\partial \tilde{p}}{\partial \tilde{\zeta}} + \mu_{nf}\left(\frac{\partial^2 \tilde{u}}{\partial \tilde{\zeta}^2} + \frac{\partial^2 \tilde{u}}{\partial \tilde{\eta}^2}\right) + g\left(\rho\gamma\right)_{nf}\left(\tilde{T} - \tilde{T}_1\right), \tag{4.3}$$

Transverse momentum equation:

$$\rho_{nf}\left(\frac{\partial}{\partial \tilde{t}} + \tilde{u}\frac{\partial}{\partial \tilde{\zeta}} + \tilde{v}\frac{\partial}{\partial \tilde{\eta}}\right)\tilde{v} = -\frac{\partial \tilde{p}}{\partial \tilde{\eta}} + \mu_{nf}\left(\frac{\partial^2 \tilde{v}}{\partial \tilde{\zeta}^2} + \frac{\partial^2 \tilde{v}}{\partial \tilde{\eta}^2}\right), \tag{4.4}$$

Energy equation:

$$\left(\rho c_p\right)_{nf}\left(\frac{\partial}{\partial \tilde{t}} + \tilde{u}\frac{\partial}{\partial \tilde{\zeta}} + \tilde{v}\frac{\partial}{\partial \tilde{\eta}}\right)\tilde{T} = k_{nf}\left(\frac{\partial^2 \tilde{T}}{\partial \tilde{\zeta}^2} + \frac{\partial^2 \tilde{T}}{\partial \tilde{\eta}^2}\right) + \tilde{Q}_0, \tag{4.5}$$

In above equations $\tilde{u}$ axial velocity, $\tilde{v}$ transverse velocity, $\tilde{\eta}$ transverse coordinate, $\tilde{T}$ is the temperature, $\tilde{Q}_0$ constants heat absorption parameter, ρ_{nf} is the nanofluid density, k_f is the thermal conductivity of the fluid, g is the acceleration due to gravity, $\tilde{p}$ is pressure, $\tilde{T}_1$ is wall temperature, γ_{nf} is the thermal expansion coefficient and $\left(\rho c_p\right)_{nf}$ is the heat capacitance.

To linearize the boundary value problem, a set of dimensionless parameters are given below:

$$\xi = \frac{\tilde{\zeta}}{\lambda}, \eta = \frac{\tilde{\eta}}{a_0}, t = \frac{c\tilde{t}}{\lambda}, u = \frac{\tilde{u}}{c}, v = \frac{\tilde{v}}{c\delta}, p = \frac{\tilde{p}a_0^{\,2}}{\mu c \lambda}, h = \frac{\tilde{h}}{a_0} = 1 + \frac{\alpha\xi}{\delta} - \varepsilon \cos \pi(\xi - t),$$

$$\delta = \frac{a_0}{\lambda}, \varphi = \frac{b}{a_0}, \theta = \frac{\tilde{T} - \tilde{T_1}}{\tilde{T_1}}, \mathrm{Re} = \frac{\rho_f c a_0}{\mu_f}, Gr_T = \frac{g\gamma_f \rho_f a_0^{\,3}\tilde{T_1}}{v_f^{\,2}}, \beta = \frac{\tilde{Q}_0 a_0}{k_f \tilde{T_1}}.$$

(4.6)

Where $\delta, \varepsilon, v, \theta, \phi, \mathrm{Re}, Gr_T, \beta$ are non-dimensional wave number, amplitude ratio, kinematic viscosity, dimensionless temperature, rescaled nanoparticle volume fraction, Reynolds number, thermal Grashof number and heat absorption parameter respectively. Under the long wavelength approximation (i.e. peristaltic wavelength is much greater than channel width, viz, $\lambda > a$, it follows that $\delta \to 0$ and also the Reynolds number vanishes ($\mathrm{Re} \to 0$). Prescribing $\delta \to 0$ negates conduit curvature effects and $\mathrm{Re} \to 0$ negates convective inertial forces relative to viscous hydrodynamic forces. Implementing these approximations, it follows that Equations $(4.2) - (4.6)$ become:

$$\frac{\partial u}{\partial \xi} + \frac{\partial v}{\partial \eta} = 0,$$

(4.7)

$$\frac{\partial p}{\partial \xi} = \frac{\mu_{nf}}{\mu_f} \frac{\partial^2 u}{\partial \eta^2} + Gr_T \frac{(\rho\gamma)_{nf}}{(\rho\gamma)_f} \theta,$$

(4.8)

$$\frac{\partial p}{\partial \eta} = 0,$$

(4.9)

$$\frac{\partial^2 \theta}{\partial \eta^2} + \beta \frac{k_f}{k_{nf}} = 0,$$

(4.10)

The relevant boundary conditions are specified as follows:

$$\frac{\partial \theta}{\partial \eta}(\xi, \eta, t)\bigg|_{\eta=0} = 0, \theta(\xi, \eta, t)\big|_{\eta=h} = 0,$$

(4.11)

$$\frac{\partial u}{\partial \eta}(\xi, \eta, t)\bigg|_{\eta=0} = 0, \ u(\xi, \eta, t)\big|_{\eta=h} = 0,$$

(4.12)

$$v(\xi, \eta, t)\big|_{\eta=0} = 0, \ v(\xi, \eta, t)\big|_{\eta=h} = \frac{\partial h}{\partial t},$$

(4.13)

34

$$p|_{\xi=0} = p_0, \ p|_{\xi=l} = p_l, \tag{4.14}$$

The thermo physical properties of the nanofluids [17] are defined as follows:

$$(\rho\gamma)_{nf} = (1-\varphi)(\rho\gamma)_f + \varphi(\rho\gamma)_s, \mu_{nf} = \frac{\mu_f}{(1-\varphi)^{2.5}}. \tag{4.15a}$$

$$k_{nf} = k_f \left(\frac{(1-\phi) + \frac{2\phi k_{CNT}}{k_{CNT}-k_f} \log\left(\frac{k_{CNT}+k_f}{2k_f}\right)}{(1-\phi) + \frac{2\phi k_f}{k_{CNT}-k_f} \log\left(\frac{k_{CNT}+k_f}{2k_f}\right)} \right). \tag{4.15b}$$

In above equations; ρ_f density of the base fluid, ρ_s density of the nanoparticles, k_f thermal conductivity of the base fluid, k_{CNT} is thermal conductivity of the single wall and multiwall carbon nanotubes, γ_{nf} is the thermal expansion coefficient, γ_f is the thermal expansion coefficient of base fluid φ is the nanoparticle volume fraction, and γ_s is the thermal expansion coefficient of the nanoparticles.

4.3. Analytical Solutions:

The analytical solutions of governing equations $(4.8) - (4.10)$ are obtained as:

$$\theta(\xi,\eta,t) = \frac{1}{2}\left[\frac{k_f}{k_{nf}}\beta(h-\eta)(h+\eta)\right], \tag{4.16}$$

$$u(\xi,\eta,t) = \frac{(\eta^2-h^2)\{\frac{k_f}{k_{nf}}\beta Gr_T\frac{(\rho\gamma)_{nf}}{(\rho\gamma)_f}(\eta^2-5h^2)\}+12\frac{dP}{d\xi}}{24(1-\varphi)^{-2.5}}. \tag{4.17}$$

To find the transverse velocity, we use the axial velocity equation (4.17) in the mass conservation equation (4.7) along with boundary condition(4.13). The expression for transverse velocity takes the form

$$v(\xi,\eta,t) = \frac{\eta h \frac{\partial h}{\partial \xi}(\frac{k_f}{k_{nf}}\beta Gr_T\frac{(\rho\gamma)_{nf}}{(\rho\gamma)_f}(\eta^2-5h^2)+6\frac{dP}{d\xi})-\eta(\eta^2-3h^2)\frac{d^2P}{d\xi^2}}{6(1-\varphi)^{-2.5}}. \tag{4.18}$$

Using the transverse vibration boundary condition leads to:

$$(1-\varphi)^{-2.5}\frac{\partial h}{\partial t} = \frac{\partial h}{\partial \xi}\left(\frac{k_f}{k_{nf}}\beta Gr_T \frac{(\rho\gamma)_{nf}}{(\rho\gamma)_f}\left(-\frac{2}{3}h^4\right)+h^2\frac{dP}{d\xi}\right)+\frac{h^3}{3}\frac{d^2P}{d\xi^2}. \tag{4.19}$$

Re-arranging and integrating equation (4.19) w.r.t. ξ gives pressure gradient:

$$\frac{\partial P}{\partial \xi} = \frac{3}{h^3}\left\{A(t)+\frac{\epsilon*\cos\pi(\xi-t)}{(1-\varphi)^{2.5}}\right\}+Gr_T\frac{(\rho\gamma)_{nf}}{(\rho\gamma)_f}\left(\frac{2}{5}\frac{k_f}{k_{nf}}\beta h^2\right), \tag{4.20}$$

Integration of equation (4.20) w.r.t. ξ provides the pressure difference ΔP across the length of the channel:

$$\Delta P(\xi,t) = \int_0^\xi \frac{3}{h^3}\left\{A(t)+\frac{\epsilon*\cos\pi(\xi-t)}{(1-\varphi)^{2.5}}\right\}+Gr_T\frac{(\rho\gamma)_{nf}}{(\rho\gamma)_f}\left(\frac{2}{5}\frac{k_f}{k_{nf}}\beta h^2\right)d\xi. \tag{4.21}$$

Upon substituting $\Delta P(\xi,t) = p(\xi,t)-p(0,t)$ and $\xi = l$, and using the finite length condition, we obtain:

$$p_l - p_0 = \int_0^l \left\{\frac{3}{h^3}\left\{A(t)+\frac{\epsilon*\cos\pi(\xi-t)}{(1-\varphi)^{2.5}}\right\}+Gr_T\frac{(\rho\gamma)_{nf}}{(\rho\gamma)_f}\left(\frac{2}{5}\frac{k_f}{k_{nf}}\beta h^2\right)\right\}d\xi. \tag{4.22}$$

Where $A(t)$ is evaluated by re-arranging the above integral and using appropriate integration techniques in Mathematica 10.0 software:

$$A(t) = \frac{(p_l-p_0)-\int_0^l\left[\frac{3\epsilon\cos\pi(\xi-t)}{h^3(1-\varphi)^{2.5}}\right]d\xi-Gr_T\frac{(\rho\gamma)_{nf}}{(\rho\gamma)_f}\left[\frac{2}{5}\frac{k_f}{k_{nf}}\beta\int_0^l h^2 d\xi\right]}{\int_0^l\frac{3}{h^3}d\xi}. \tag{4.23}$$

4.4. Graphical Representation and Discussion:

To observe the effective thermal conductivity of the fluid with single wall carbon nanotube (SWCnt) and multiwall carbon nanotube (MWCnt), we fixed all the other constraints to a constant value and observed that the thermal conductivity is higher for SWCNT and slightly lesser for MWCnt as shown in Fig. 4.2. This can be depicted in Fig. 4.3 where the temperature rise is marginally greater in case of MWCnt's and slightly lesser in case of SWCnt's. Note that the

temperature rise is directly proportional to the heat absorption parameter β. However, the rise in temperature is greater in case of a non-uniform channel.

From Fig. 4.4, we observe that the axial velocity $u(\xi,\eta)$ increases with an increase in both β and G_{rT}. MWCnt attains higher axial velocity as compared to the SWCnt in all cases but the increase in velocity is slightly greater in case of uniform channel. Velocity is maximum at the center of the tube where $\eta = 0$. The transverse velocity $v(\xi,\eta)$ and its variation for heat absorption parameter and thermal Grashof number is shown in Fig. 4.5. The transverse velocity carries similar features as that of the axial velocity except that it is minimum at the center of the tube where $\eta = 0$. We have noticed that MWCnt's have this exceptional quality to increase the axial velocity as well as the transverse velocity of the governing fluids.

Fig. 4.6 depicts that pressure gradient has a sinusoidal behavior. It is directly proportional to the thermal Grashof number. For non-uniform channel i.e. $\alpha \neq 0$, the pressure gradient increases as we increase the length of the channel.

Figs.4.7, 4.8 (a, b) shows the streamlines for different values of heat absorption parameter β for SWCnt and MWcnt it is seen that by increasing β, number of bolus increases and size of the bolus decreases for SWCnt but for the case of MWCnt results are different, by increasing β number of bolus decreases and size of the of the bolus increases.

Figs. 4.9, 4.10 (a, b) present the streamlines for different values of Grashof number Gr_T for SWCnt and MWcnt it is observed that increasing Grashof number Gr_T size of the of the bolus decreases for SWCnt as well as for the case of MWCnt.
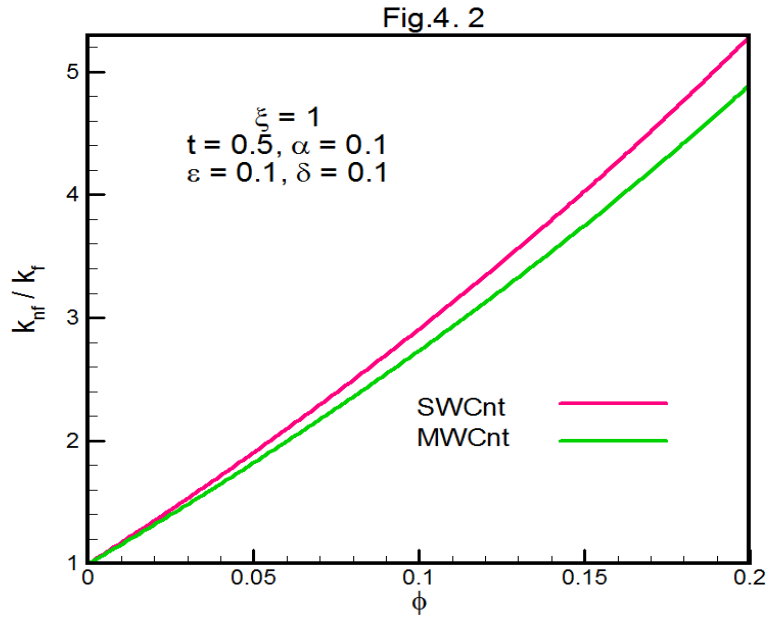
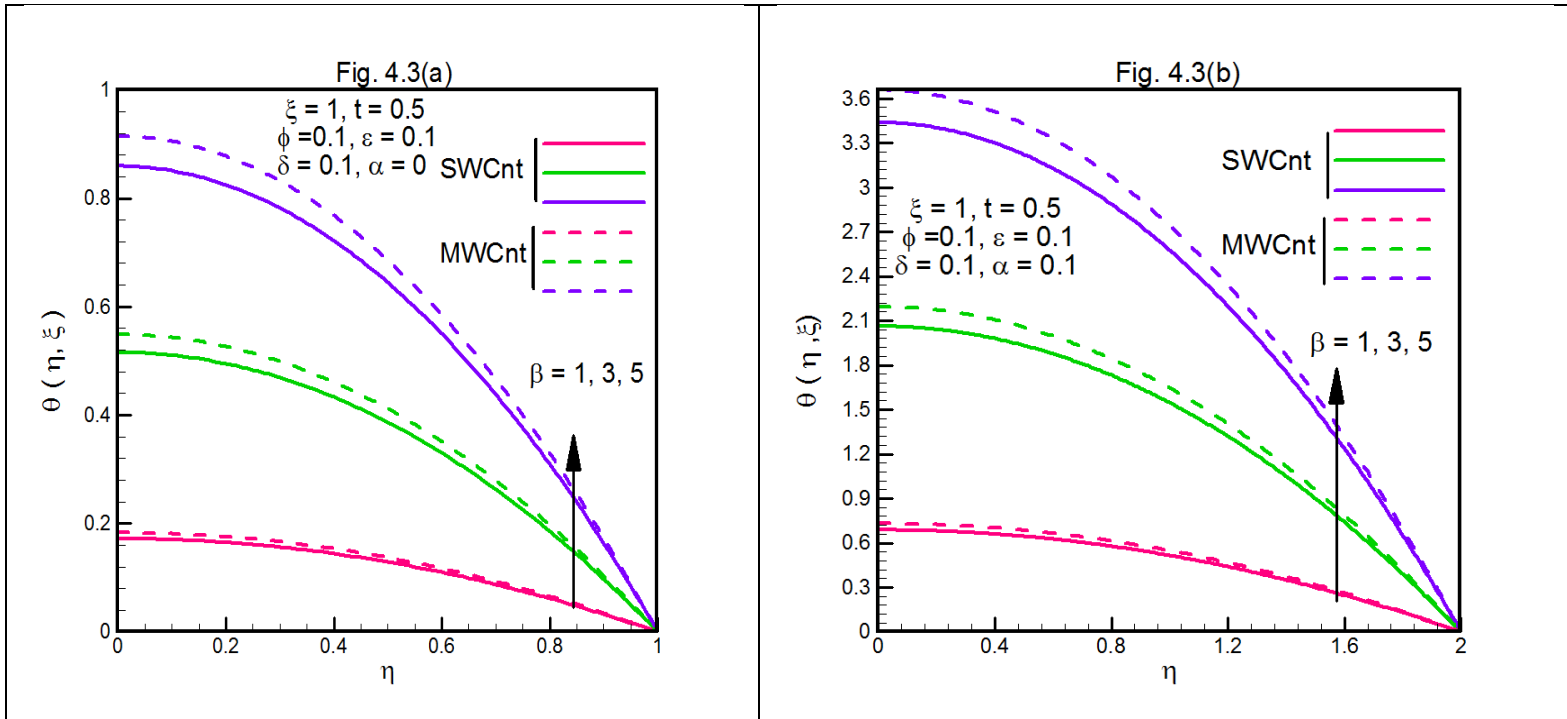Fig. 4.2 Effective thermal conductivity of the nanofluid $\frac{k_{nf}}{k_f}$ for SWCnt and MWCnt.

Fig. 4.3 Temperature profile ($\theta(\xi, \eta)\ vs\ \eta$) for various value of (a) heat absorption parameter β

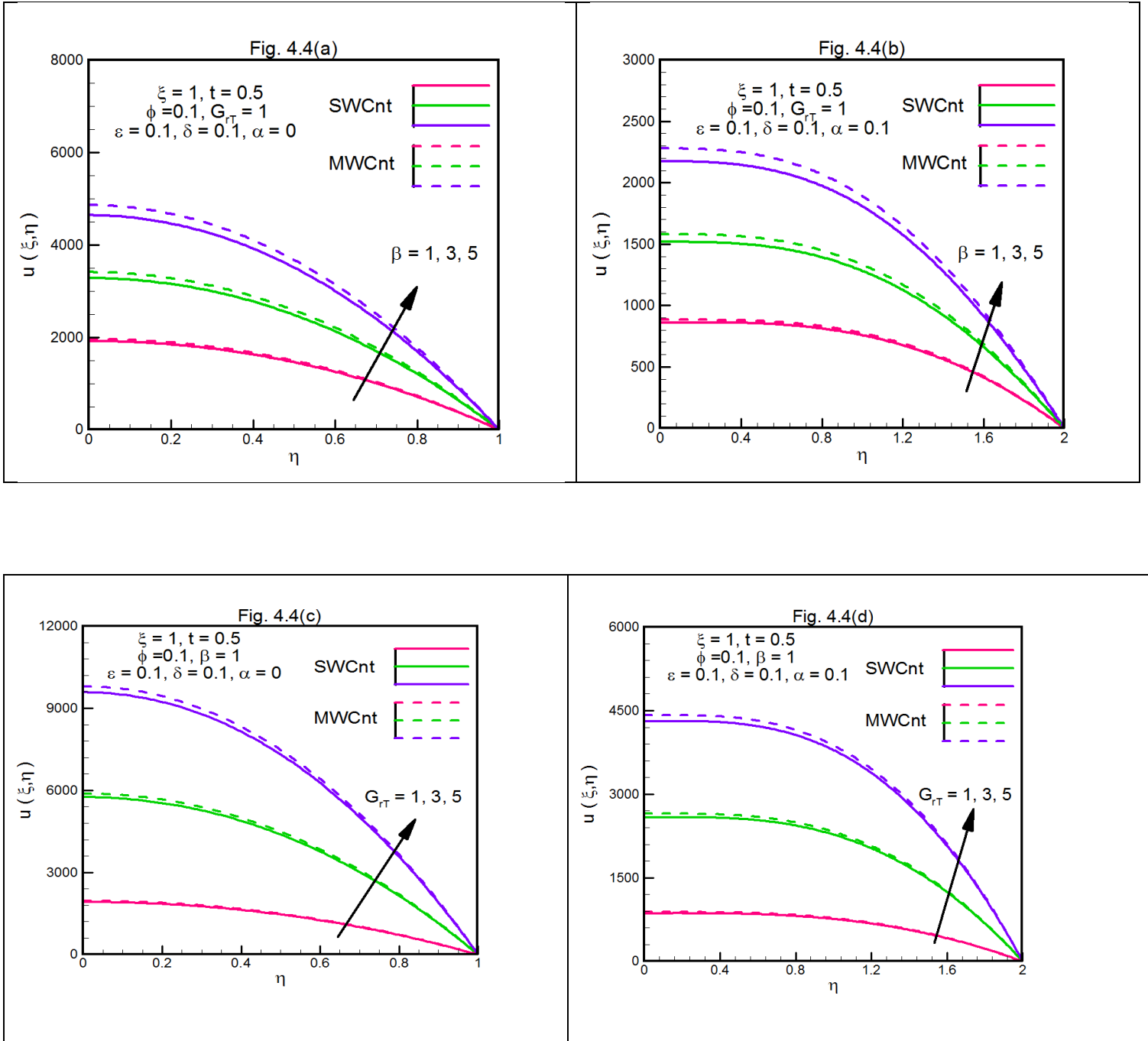in uniform channel $\alpha = 0$, (b) heat absorption parameter β in a non-uniform channel $\alpha = 0.1$.

Fig. 4.4 Axial velocity profile ($u(\xi,\eta)$ vs η) for various value of (a) Heat absorption parameter β in a uniform channel $\alpha = 0$. (b) Heat absorption parameter β in a non-uniform channel $\alpha = 0.1$. (c) Grashof number Gr_T in uniform channel $\alpha = 0$. (d) Grashof number Gr_T in a non-uniform channel $\alpha = 0.1$.
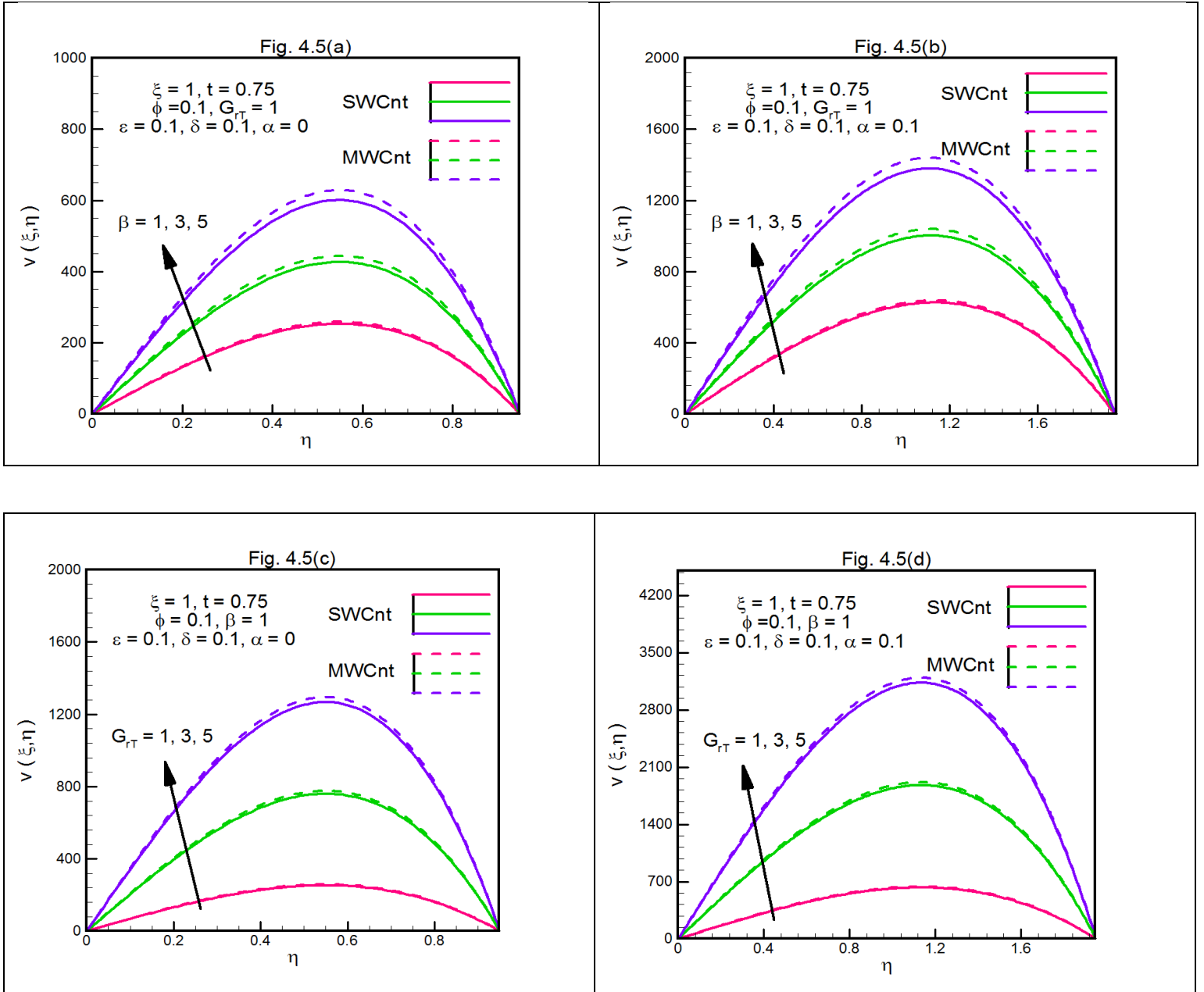
Fig. 4.5 Transverse velocity profile ($v(\xi,\eta)$ vs η) for various value of (a) Heat absorption parameter β in uniform channel $\alpha = 0$. (b) Heat absorption parameter β in a non-uniform channel $\alpha = 0.1$. (c) Grashof number Gr_T in uniform channel $\alpha = 0$. (d) Grashof number Gr_T in a non-uniform channel $\alpha = 0.1$.
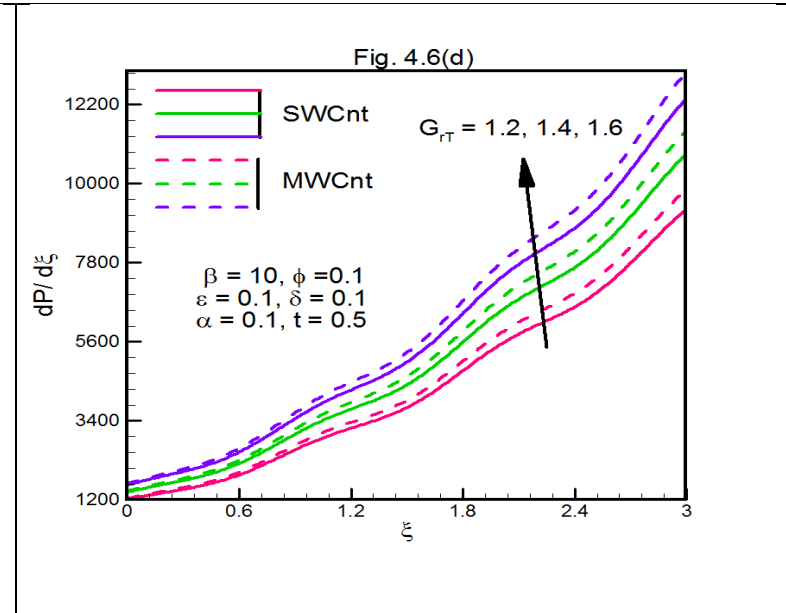
Fig. 4.6 Pressure difference for various values of (a) Heat absorption parameter β in uniform channel $\alpha = 0$. (b) Heat absorption parameter β in a non-uniform channel $\alpha = 0$. (c) Grashof number Gr_T in uniform channel $\alpha = 0$, (d) Grashof number Gr_T in and non-uniform channel $\alpha = 0.1$.
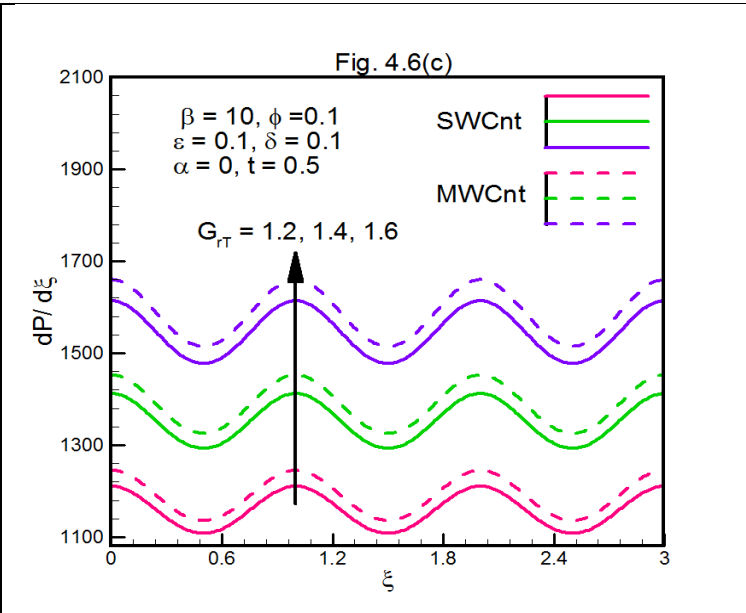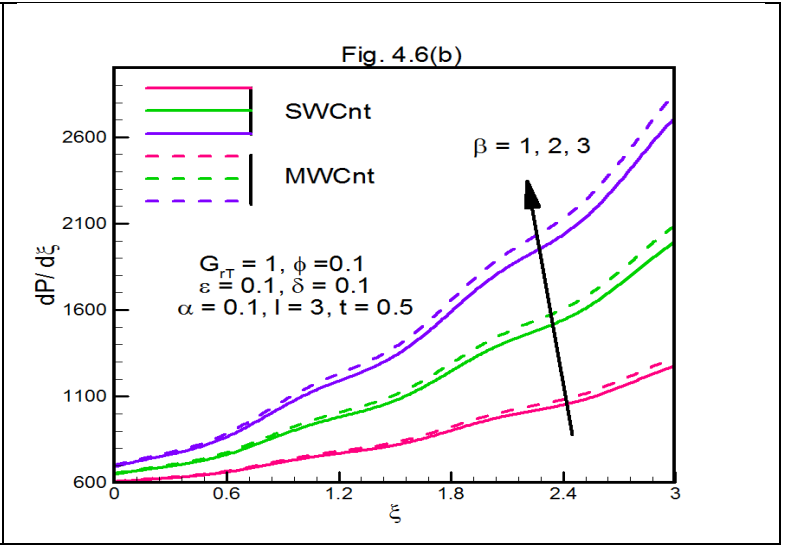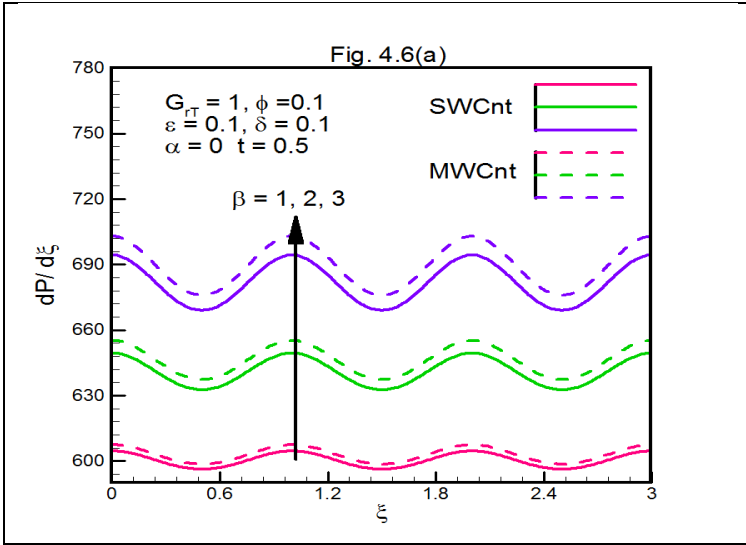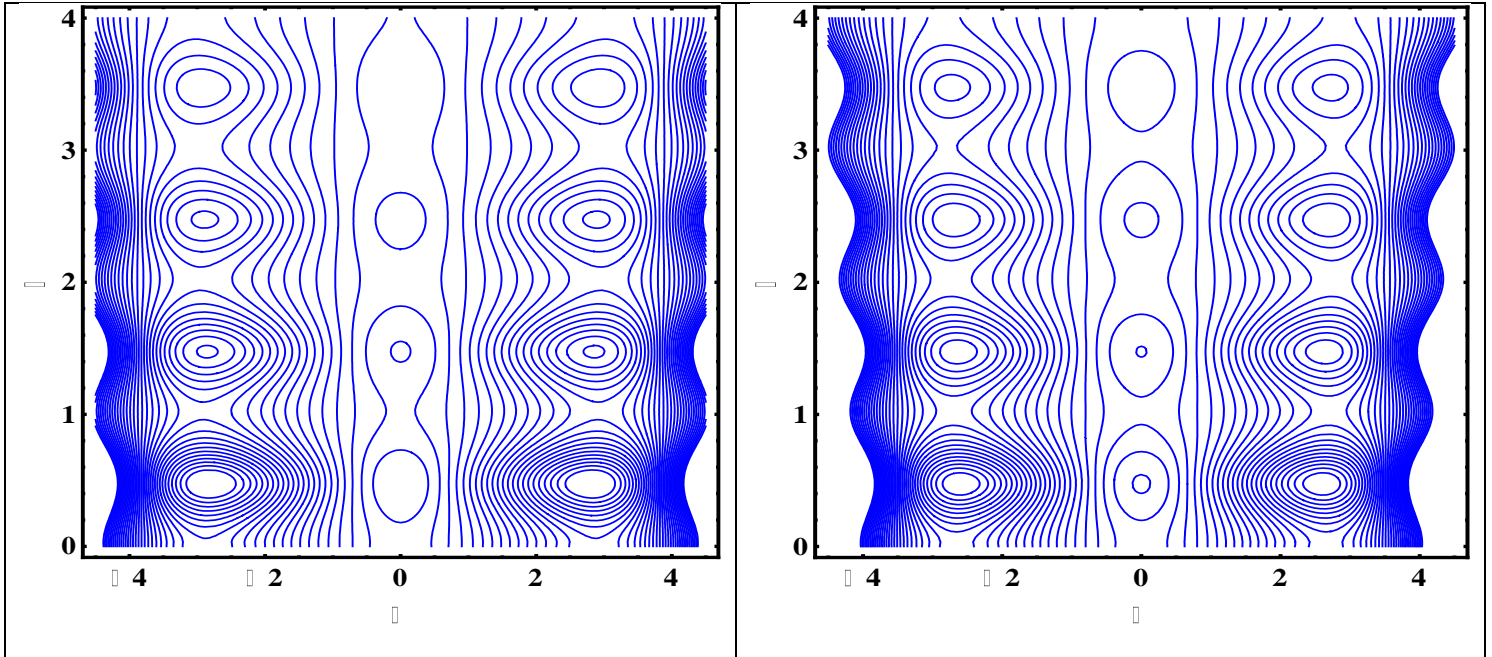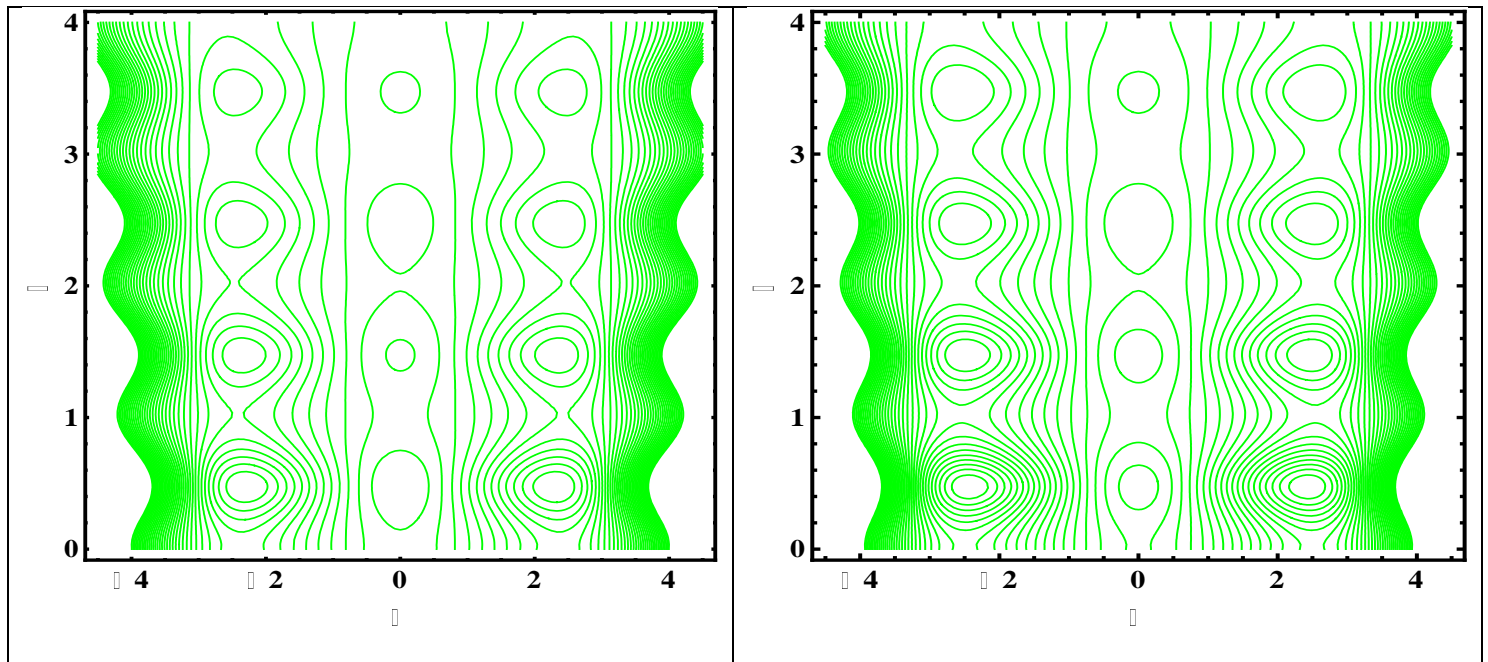
Figs. 4.7 Streamlines (SWCnt) for various values of β. (a) $\beta = 0.5$. (b) $\beta = 0.8$.   other parameters

are $Gr_T = 0.5$, $\alpha = 0.4$, ϕ = 0.2, ε = 0.3, δ = 0.1, t = 0.5.

Figs. 4.8 Streamlines (MWCnt) for various values of β. (a) $\beta = 0.5$. (b) $\beta = 0.8$.   other

parameters are $Gr_T = 0.5$, $\alpha = 0.4$, ϕ = 0.2, ε = 0.3, δ = 0.1, t = 0.5.
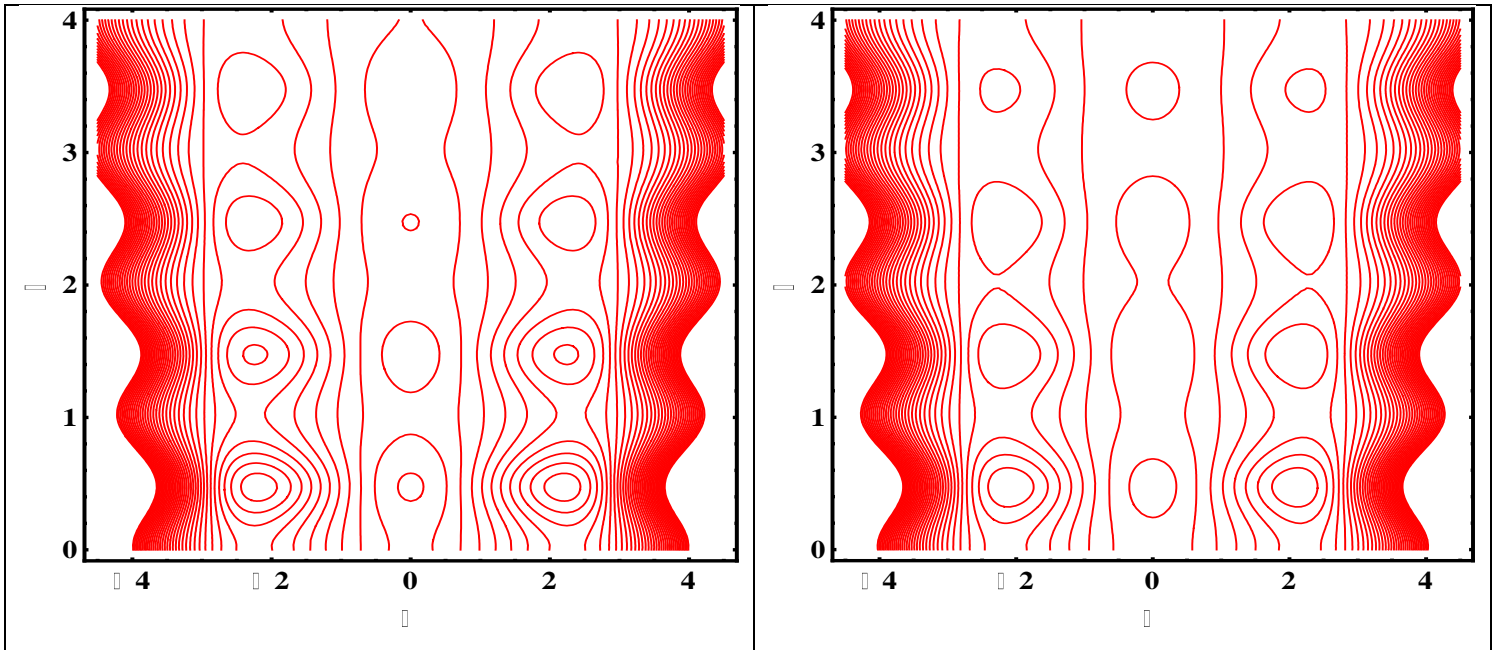
Figs.4.9 Streamlines (SWCnt) for various values of Gr_T. (a) $Gr_T = 0.3$. (b) $Gr_T = 0.6$, $\beta = 0.5$,
$\alpha = 0.4$, φ = 0.2, ε = 0.3, δ = 0.1, t = 0.5.

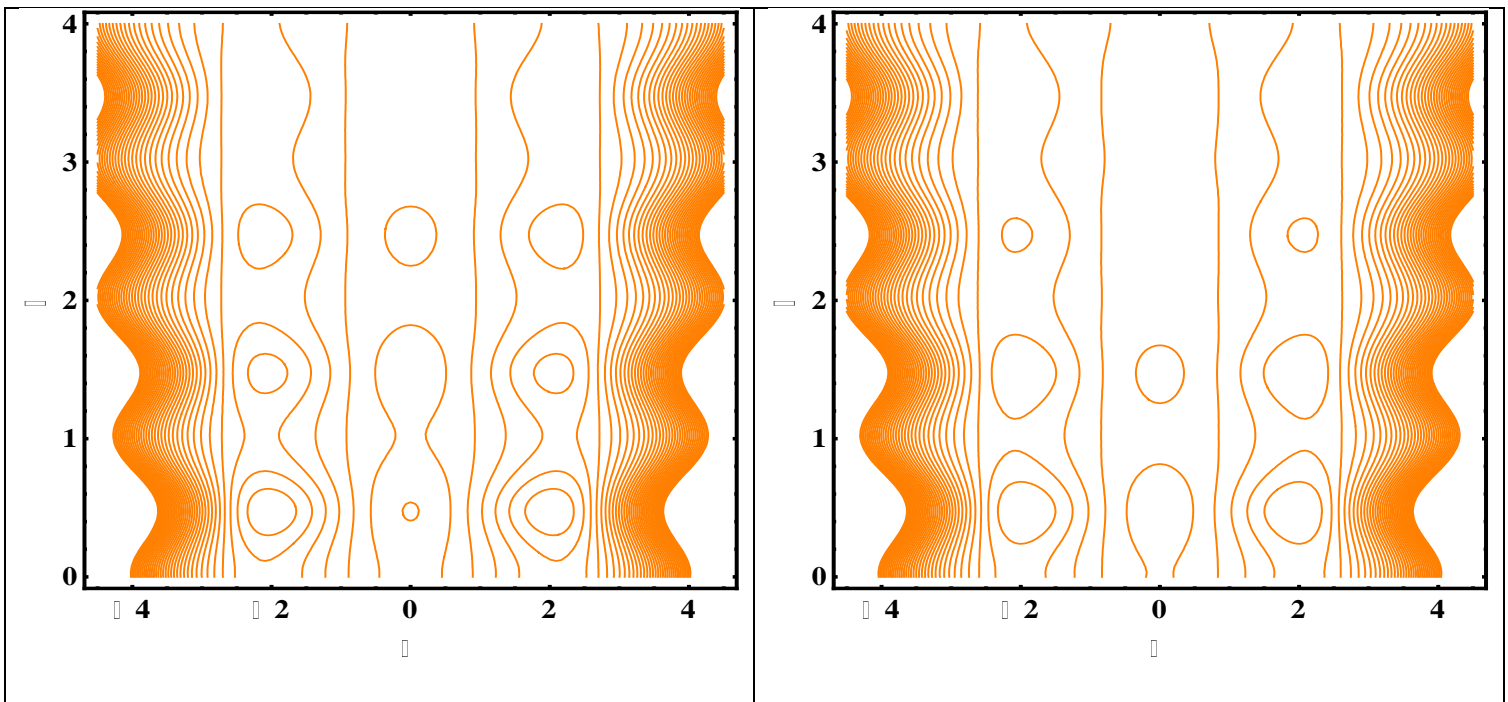Figs 4.10 Streamlines (MWCnt) for various values of Gr_T. (a) $Gr_T = 0.3$. (b) $Gr_T = 0.6$.   other
parameters are $\beta = 0.5$, $\alpha = 0.4$, φ = 0.2, ε = 0.3, δ = 0.1, t = 0.5.

Conclusions:

1. Thermal conductivity is higher for single wall carbon nanotubes.

2. Temperature rise is marginally greater in case of multi wall carbon nanotubes.

3. Axial velocity increases with an increase in both the heat absorption parameter and the thermal grashof number

4. The pressure difference reduces by increasing Brownian motion parameter N_b. The pressure difference is increased by increasing thermophoresis parameter N_t.

6. The pressure difference reduces by increasing the values of heat absorption parameter and thermal Grashof number.

7. Number of trapped bolus increases by increasing heat absorption parameter and number of trapped bolus is decreased by increasing heat absorption parameter

8. Size of boluses decreases by decreasing increasing thermal Grashof number.

9. Size of boluses decreases by increasing thermal Grashof number.

References:

1.   Shapiro AH, Jaffrin MY, Weinberg SL (1969) Peristaltic pumping with long wavelengths at low Reynolds number. J Fluid Mech 37(4):799-825.

2.   Radhakrishnamacharya G (1982) Long wavelength approximation to peristaltic motion of a power law fluid. Rheol Acta 21(1):30-35.

3.   Srivastava LM (1985) Flow of couple stress fluid through stenotic blood vessels. J Biomech, 18(7):479-485.

4.   Pozrikidis C (1987) A study of peristaltic flow. J Fluid Mech 180:515-527.

5.   Li M, Brasseur JG (1993) Non-steady peristaltic transport in finite-length tubes. J Fluid Mech, 248:129-151.

6.   Wang XQ, Mujumdar AS (2007) Heat transfer characteristics of nanofluids: a review. Int J Therm Sci 46(1):1-19.

7.   Cremer J, Segota I, Yang CY, Arnoldini M, Sauls JT, Zhang Z, Gutierrez E, Groisman A, Hwa T (2016) Effect of flow and peristaltic mixing on bacterial growth in a gut-like channel. P Natl Acad Sci USA 113(41):11414:11419.

8.   Bhatti MM, Abbas MA, Rashidi MM (2016) Analytic Study of Drug Delivery in Peristaltically Induced Motion of Non-Newtonian Nanofluid. J Nanofluids 5(6):920-927.

9.   Bhatti MM, Zeeshan A, Ellahi R (2016) Heat transfer analysis on peristaltically induced motion of particle-fluid suspension with variable viscosity: Clot blood model. Comput Meth Prog Bio 137:115-124.

10.   Yu W, France DM, Routbort JL, Choi SU (2008) Review and comparison of nanofluid thermal conductivity and heat transfer enhancements. Heat Transfer Eng 29(5):432-460.

11.   Kakac S, Pramuanjaroenkij A (2009) Review of convective heat transfer enhancement with nanofluids. Int J Heat Mass Tran 52(13-14):3187-3196.

12.   Özerinç S, Kakaç S, Yazıcıoğlu AG (2010) Enhanced thermal conductivity of nanofluids: a state-of-the-art review. Microfluid Nanofluid 8(2):145-170.

13.   Akbar NS, Butt AW, Noor NFM (2014) Heat Transfer Analysis on Transport of Copper Nanofluids Due to Metachronal Waves of Cilia. Curr Nanosci 10(6):807-815.

14.   Akbar NS, Maraj EN, Butt AW (2014) Copper nanoparticles impinging on a curved channel with compliant walls and peristalsis. Eur Phys J Plus 129:183.

15.   Abdul Khaliq R, Kafafy R, Salleh HM, Faris WF (2012) Enhancing the efficiency of polymerase chain reaction using graphene nanoflakes. Nanotechnology 23(45): 455106.

16.   Mahian O, Kianifar A, Kalogirou SA, Pop I, Wongwises S (2013) A review of the applications of nanofluids in solar energy. Int J Heat Mass Tran 57(2):582-594.

17.   Akbar NS, Butt AW (2015) Carbon nanotubes analysis for the peristaltic flow in curved channel with heat transfer. Appl Math Comput 259:231-241.

18.   Akbar NS, Butt AW (2016) Carbon nanotube (CNT) suspended nanofluid analysis due to metachronal beating of cilia with entropy generation. J Braz Soc Mech Sci & Eng 2016:1-12.

19.   Ellahi R, Rahman SU, Nadeem S, Akbar NS (2014) Influence of Heat and Mass Transfer on Micropolar Fluid of Blood Flow Through a Tapered Stenosed Arteries with Permeable Walls. J Comput Theor Nanosci 11(4):1156-1163.

20.   Bhatti MM, Ellahi R, Zeeshan A (2016) Study of variable magnetic field on the peristaltic flow of Jeffrey fluid in a non-uniform rectangular duct having compliant walls. J Mol Liq 222:101-108.

21.   Ellahi R, Hassan M, Zeeshan A (2015) Shape effects of nanosize particles in Cu-H_2O nanofluid on entropy generation. Int J Heat Mass Tran 81:449-456.

22.   Ellahi R, Hassan M, Zeeshan A, Khan AA (2016) Shape effects of nanoparticles suspended in HFE-7100 over wedge with entropy generation and mixed convection. Appl Nanosci 6(5):641-651.

23.   Ellahi R, Zeeshan A, Hassan M (2016) Particle shape effects on marangoni convection boundary layer flow of a nanofluid. Int J Numer Method H 26(7):2160-2174.

24.   Ellahi R, Hassan M, Zeeshan A (2015) Study on magnetohydrodynamic nanofluid by means of single and multi-walled carbon nanotubes suspended in a salt water solution, IEEE Transactions on Nanotechnology. 14 (4):726 – 734.

25.   Akbar NS, Nadeem S,Hayat T, Hendi AA (2012) Study of Peristaltic flow of a nanofluid in a non-uniform tube, Heat mass transfer 48:451 – 459.

26.   Zueco J, Prasad VR, Beg OA, Takhar HS (2011) Study of thermophoretic hydromagnetic dissipative heat and mass transfer with lateral mass flux, heat source, ohmic heating and thermal conductivity effects.29:2808 – 2815.

27.   Kuznetsov AV, Nield DA (2010) Study of Natural convective boundary-layer flow of a nanofluid past a verticle plate. Int J therm Sci 49:243 – 247.

28. Fung YC, Yih CS (1968) Study of peristaltic transport. ASME J Appl Mech 35: 669 – 675

29. Tripathi D, A mathematical model for swallowing of food bolus through the oesophagus under the influence of heat transfer, Int. J. Therm. Sci. 51 (2012) 91–101.

30. Nield DA, Kuznetsov AV, The onset of double-diffusive convection in a nanofluid layer, Int. J. Heat Fluid Flow 32 (2011) 771–776.

31. Pandey SK, Tripathi D, Influence of magnetic field on the peristaltic flow of a viscous fluid through a finite-length cylindrical tube, Appl. Bionics Biomech. 7 (2010) 169–176.

32. Tripathi D, A mathematical model for the peristaltic flow of chyme movement in small intestine, Math. Biosci. 233 (2011) 90–97.

33. Tripathi D, Numerical study on creeping flow of Burgers' fluids through a peristaltic tube, ASME J. Fluids Eng. 133 (2011) 121104-1–121104-9.

34. Tripathi D, Numerical study on peristaltic flow of generalized Burgers' fluids in uniform tubes in presence of an endoscope, Int. J. Numer. Methods Biomed. Eng. 27 (2011) 1812–1828.

35. Tripathi D, Peristaltic transport of fractional Maxwell fluids in uniform tubes: application of an endoscope, Comput. Math. Appl. 62 (2011) 1116– 1126.

36. Tripathi D, Numerical study on peristaltic transport of fractional bio-fluids, J. Mech. Med. Biol. 11 (2011) 1045–1058

37. Beg OA, Prasad VR, Vasu B, Reddy NB, Li Q, Bhargava R, Free convection heat and mass transfer from an isothermal sphere to a micropolar regime with Soret/Dufour effects, Int. J. Heat Mass Transfer 54 (2011) 9–18.

38. J.Buongiorno,Convective transport in nanofluids,ASME J.Heat Transfer 128(2006) 240–250.

39. A.V. Kuznetsov, D.A. Nield, Natural convective boundary-layer flow of a nanofluid past a vertical plate, Int. J. Therm. Sci. 49 (2010) 243–247.

40. Q. Xue. Model for thermal conductivity of carbon nanotube-based composites. Modern Phys. Lett. B, 368(2005)302–307

41. Tripathi D, Beg OA, A study on peristaltic flow of nanofluids: Application in drug delivery systems, Int J Heat Mass Tran 70(2014)61–70.

42. Akbar NS, Ayub A, Butt AW, Carbon nanotube analysis for an unsteady physiological flow in a non-uniform channel of finite length, Eur. Phys. J. Plus (2017) 132– 177.